Anales Acad. Nac. de Cs. Ex., Fís. y Nat., tomo 53 (2001): 84-120.

PHOTOREACTOR ANALYSIS THROUGH TWO EXAMPLES IN ADVANCED OXIDATION TECHNOLOGIES

Alberto E. Cassano and Orlando M. Alfano

INTEC (Universidad Nacional del Litoral and CONICET).
Güemes 3450, (3000) Santa Fe, Argentina. E-mail: acassano@ceride.gov.ar

Abstract

This paper presents the most important technical tools that are needed for designing homogeneous and heterogeneous photoreactors using computer simulation of a rigorous mathematical description of the reactor performance. Employing intrinsic reaction kinetic models and parameters derived from properly analyzed laboratory information, it is shown that is possible to scale up reactors with no additional information and without resorting to empirically adjusted correcting factors. The method is illustrated with two examples concerning the degradation of organic pollutants as typical applications of the newly developed Advanced Oxidation Technologies. One particular aspect of heterogeneous photoreactors gives to these reactions a unique characteristic: in many cases, absorption of light by the solid can not be separated from scattering or reflection by the catalyst, turning more difficult the analysis of kinetic information and the design of practical reactors. This paper describes in a very succinct manner the way to perform a rigorous analysis of some of these reactors. Starting always from fundamental principles and using mathematical modeling as the main tool, we show the methods to tackle all problems derived from the most difficult type of system heterogeneities. Two reactors are modeled to show the proposed approach. In the case of homogeneous reactions, predictions from the model are compared with experimental data obtaining reasonable good results. They provide confidence on mathematical modeling as a design methodology for homogeneous photochemical reactors. In the case of heterogeneous reactions, the procedure is illustrated with the design and analysis of a laboratory reactor. The objective is the acquisition of kinetic parameters that must be independent of the reactor geometry, size and form of illumination.

Key words: Photochemical reactors, Radiation field, Homogeneous photoreactions, Heterogeneous photoreactions.

Trabajo presentado con motivo de la entrega del premio "Gustavo Fester" en Ingeniería Química, al Dr. Alberto E. Cassano, el 10 de noviembre de 2000.

Resumen

Este trabajo describe las herramientas técnicas más importantes que se requieren para diseñar fotorreactores homogéneos y heterogéneos empleando la simulación computacional de descripciones matemáticas rigurosas de la *performance* del reactor. Empleando modelos cinéticos intrínsecos de reacción y parámetros derivados de experimentos de laboratorio adecuadamente analizados, se muestra cómo es posible hacer cambios de escala sin necesidad de información adicional o el empleo de factores de corrección empíricamente ajustados. El método se ilustra con dos ejemplos que abordan la degradación de contaminantes orgánicos como una aplicación típica de las recientemente desarrolladas Tecnologías Avanzadas de Oxidación. Un aspecto particular de los reactores heterogéneos provee a estas reacciones de características únicas: en muchos casos la absorción de radiación por el sólido no puede ser separada de la dispersión de la radiación por el catalizador lo que vuelve mucho más complejo el análisis de la información cinética y el diseño de reactores prácticos. Esta contribución describe de una manera muy sucinta la forma de llevar a cabo un análisis riguroso de algunos de estos reactores. Partiendo siempre de principios fundamentales y usando modelado matemático como herramienta principal se muestran los métodos que se pueden emplear para tratar los problemas derivados del más dificultoso sistema con heterogeneidades. Para mostrar la metodología propuesta se modelan dos reactores. En el caso del sistema homogéneo predicciones a partir del modelo se comparan con datos experimentales propios obteniéndose una razonable concordancia. Estos resultados proveen confianza en el modelado matemático como metodología de diseño para fotorreactores homogéneos. En el caso de los fotorreactores heterogéneos el procedimiento se ilustra con el diseño de un reactor experimental de laboratorio. El objetivo en este caso es la adquisición de parámetros cinéticos que resulten independientes de la geometría, tamaño y forma de iluminación.

Palabras clave: Reactores fotoquímicos, Campo de radiación, Reacciones homogéneas, Reacciones heterogéneas.

Outline

I. Notation

a_S particle surface area (cm^2 particle^{-1})
a_V solid-liquid interfacial area per unit reactor volume (cm^2 cm^{-3})
C_i molar concentration of component i (mol cm^{-3})
C_{mp} mass catalyst concentration (g cm^{-3})
C_p specific heat at constant pressure (joule g^{-1} K^{-1})
$\mathscr{D}_{im}$ diffusion coefficient of component i in the mixture (cm^2 s^{-1})
e^a volumetric rate of photon absorption (einstein s^{-1} cm^{-3})
G incident radiation (also known as spherical irradiance) (einstein s^{-1} cm^{-2})
Ge geometric number (dimensionless)
h film heat transfer coefficient (joule cm^{-2} s^{-1} K^{-1}); also Planck constant (joule s)
H_i enthalpy of component i (joule mol^{-1})
ΔH heat of reaction at constant pressure (joule mol^{-1})
I specific (radiation) intensity (also known as radiance) (einstein s^{-1} cm^{-2} sr^{-1})
j^e radiation emission (einstein s^{-1} cm^{-3} sr^{-1})

$\underline{J}_i$	molar diffusive density flux vector of component i (mol s^{-1} cm^{-2})
k	kinetic constant (for different reaction steps) (units vary with type of step)
k_e	thermal conductivity (joule cm^{-1} s^{-1} K^{-1})
L	length (cm)
L_L	lamp length (cm)
LVRPA	local volumetric rate of photon absorption (einstein s^{-1} cm^{-3})
$\mathcal{N}_{\lambda,\underline{\Omega}}$	λ, $\underline{\Omega}$ photon density number (photons cm^{-3} sr^{-1} and unit wavelength interval)
$\underline{n}$	unit normal vector to a given surface
N	number of particles
N_V	number of particles per unit volume (particle cm^{-3})
$\underline{N}_i$	molar flux of component i (mol cm^{-2} s^{-1})
Nu	Nusselt number (dimensionless)
p	phase function (dimensionless)
P	output power from the lamp (einstein s^{-1})
Pe_i	radial Peclet number for mass (dimensionless)
Pe_T	radial Peclet number for heat (dimensionless)
q	radiation density flux for a given direction or surface orientation (also known as superficial irradiance) (einstein s^{-1} cm^{-2})
$\underline{q}$	radiation density flux vector (einstein s^{-1} cm^{-2})
Q^{Ext}	heat transferred from external fields (joule g^{-1} s^{-1})
Q_R	dimensionless heat of reaction
r	radius (cm) or radial coordinate (cm)
R_L	lamp radius (cm)
$R_{Hom,i}$	homogeneous, molar reaction rate of component i (mol cm^{-3} s^{-1})
$R_{Het,i}$	heterogeneous, molar reaction rate of component i (mol cm^{-2} s^{-1})
s	variable representing distances in a 3-D space (cm)
S_g	catalyst specific surface area (cm^2 g^{-1})
t	time (s)
T	temperature (K)
U	dimensionless axial velocity
v	velocity (cm s^{-1})
V	volume (cm^3)
VRPA	some average of the LVRPA (einstein s^{-1} cm^{-3})
x	cartesian coordinate (cm)
$\underline{x}$	vector representing position in a 3-D space (cm)
y	cartesian coordinate (cm)
z	cartesian or cylindrical coordinate (cm)

Greek letters

β	cylindrical coordinate (rad)
β	extinction coefficient = $\kappa + \sigma$ (cm^{-1})
γ	dimensionless radial coordinate
ε	liquid hold-up (dimensionless)
ζ	dimensionless axial coordinate; also 3-D position vector inside a material particle (cm)
θ	spherical coordinate (rad)
κ	absorption coefficient (cm^{-1})
κ^*	specific (per unit mass) absorption coefficient (cm^2 g^{-1})
λ	wavelength (nm = 10^{-7} cm)
μ	direction cosine $\mu = \cos\theta$
ν	frequency (s^{-1})
ρ	interfacial reflectivity (dimensionless)
ρ_{mix}	density of mixture (g cm^{-1})
σ	scattering coefficient (cm^{-1})
σ^*	specific (per unit mass) scattering coefficient (cm^2 g^{-1})
χ	characteristic constant of the annular space (dimensionless)
τ	dimensionless temperature
Y	transmission or compounded transmission coefficient (dimensionless)
ϕ	spherical coordinate (rad)
Φ	overall quantum yield (mol $einstein^{-1}$)
Ψ_i	dimensionless concentration of component i
Ω	solid angle (sr, ster radian)
Ω_i	dimensionless reaction rate of component i
$\underline{\Omega}$	unit vector in the direction of radiation propagation

Superscripts

a	denotes absorbed energy

Dir denotes direct radiation from the lamp
Pseudo denotes a heterogeneous reaction expressed per unit reactor volume
0 denotes initial or inlet conditions
Ref denotes reflected radiation from the reflector
* denotes specific (per unit mass) properties

Subscripts

A denotes area
Ac denotes actinometer
Hom denotes a homogeneous reaction
Het denotes a heterogeneous reaction
i denotes internal or component i
L denotes liquid phase
o denotes outside or external
0 denotes initial value or inlet condition
R denotes reactor
r denotes radius or radial direction
S denotes solid phase
Sol denotes solid surface
Susp denotes suspension
T denotes total
Tk denotes tank
V denotes volume
z denotes axial direction
λ denotes wavelength
Σ denotes polychromatic radiation
Ω denotes direction of radiation propagation

Special Symbols

_ denotes vector value
⟨ ⟩ denotes average value

II. Scope and limitations

A short work to discuss Reactor Analysis in Advanced Oxidation Technologies (AOTs) is an impossible task unless we decide that the readers of this paper have a previous background on the subject and related transport phenomena (a good undergraduate level in chemical engineering seems appropriate) [Froment and Bischoff, 1990; Bird *et al.*, 2002]. Moreover, we can increase its feasibility if coverage is restricted to only a fraction, albeit significant, of AOTs namely homogeneous and heterogeneous photoreactions. On these premises, it is possible to concentrate our effort in those aspects that are distinctive of photochemical and photocatalytic processes.

The distinct aspect of these reactions is the unavoidable existence of a radiation field inside the reactor, that only in very special cases can be considered uniform in space and frequently is not even constant in time. These **intrinsic non-uniformities,** often neglected, are responsible for the majority of the difficulties associated with photoreactor analysis and design.

Many different shapes and configurations are possible for either single phase or multiphase reactors [Cassano *et al.*, 1995; Braun *et al.*, 1993; Puma and Yue, 1998; Ray, 1998; Cassano and Alfano, 2000]. Again, we will restrict ourselves to describe in more details only a few of them.

III. Mass and energy balances

III.1. *Mass conservation equations*

The general mass conservation equation is [Bird *et al.*, 2002, p 584]:

$$\underbrace{\frac{\partial C_i}{\partial t}}_{\text{Unsteady state}} + \underbrace{\nabla \cdot \underline{N}_i}_{\substack{\text{All molar fluxes} \\ \text{(Convection and Difussion)}}} = \underbrace{R_{Hom,i}}_{\text{Homogeneous Reactions}} \qquad (1)$$

Since the differential equation is valid for a single phase, only homogeneous reactions are included in Eq. (1). Heterogeneous reactions ($R_{Het,i}$) for example, in superficial, catalytic processes can be incorporated into the analysis if one considers that they are boundary conditions for Eq. (1). However, if a parallel homogeneous reaction is present, for example photocatalysis when also direct photolysis occurs, both $R_{Het,i}$ and $R_{Hom,i}$ must be included.

Equations will be derived for three representative cases: the tubular reactor of

annular cross section, the isothermal, well-mixed batch reactor, and the isothermal batch reactor in a recycle.

III.1.1. *The tubular reactor* (Fig. 1)

Consider firstly a tubular, cylindrical reactor formed by an annular space surrounding a tubular lamp. This is the simplest and more practical continuous photoreactor, particularly for artificial light illumination of a single-phase system. Under the following assumptions and operating conditions: (i) steady state; (ii) unidirectional, incompressible, continuous flow of a Newtonian fluid under fully developed laminar regime; (iii) only ordinary (concentration) diffusion is significant (i.e., pressure diffusion, forced diffusion and thermal diffusion are neglected); (iv) azimuthal symmetry, (v) axial diffusion neglected as compared to the convective flow; (vi) constant physical and transport properties, (vii) non-permeable reactor walls, and (viii) for the moment, monochromatic operation, the following equation in cylindrical coordinates holds [Bird *et al.*, 2002, p 850]:

$$\underbrace{v_z(r)\frac{\partial C_i(z,r)}{\partial z}}_{\text{Convective flow in the axial direction}} \underbrace{-\mathscr{D}_{im}\left[\frac{1}{r}\frac{\partial}{\partial r}\left(r\frac{\partial C_i(z,r)}{\partial r}\right)\right]}_{\text{Diffusional flux in the radial direction}} = \underbrace{R_{Hom,i}(z,r)}_{\text{Homogeneous reaction rate}} \qquad (2)$$

Symbols are defined in the notation section. v_z is the axial velocity in laminar flow, a function of the radial position and represented by the classical non-symmetric parabolic profile characteristic of annular spaces [Bird *et al.*, 2002, p. 55]. Usually it is very convenient to obtain the solution of this differential equation in terms of dimensionless variables and parameters. To make this equation dimensionless let us define:

$$\gamma = \frac{r}{r_{R_i}},\quad \zeta = \frac{z}{L_R},\quad Ge = \frac{r_{R_i}}{L_R},\quad U = \frac{v_z}{\langle v_z\rangle}$$

$$\psi_i = \frac{C_i}{C_K^0},\quad Pe_i = \frac{r_{R_i}\langle v_z\rangle}{\mathscr{D}_{im}},\quad \Omega_i = \frac{R_{Hom,i}\,L_R}{\langle v_z\rangle C_K^0}$$

$\langle v_z\rangle$ is the averaged velocity over the reactor cross section area and Ge is the geometric number representing the reactor slenderness, a very important parameter in photochemical reactors. Concentration is made dimensionless using some key reactant (K) initial concentration. Pe_i is the Peclet number for radial mass transport of component i and Ω_i is a dimensionless reaction rate for component i. Then, with some trivial algebra:

$$\underbrace{U(\gamma)\frac{\partial \psi_i}{\partial \zeta}}_{\text{Axial flow}} \underbrace{-\frac{1}{Pe\,Ge}\left[\frac{1}{\gamma}\frac{\partial}{\partial \gamma}\left(\gamma\frac{\partial \psi_i}{\partial \gamma}\right)\right]}_{\text{Diffusional flux along r}} = \underbrace{\Omega_i}_{\text{Reaction Rate of component i}} \qquad (3)$$

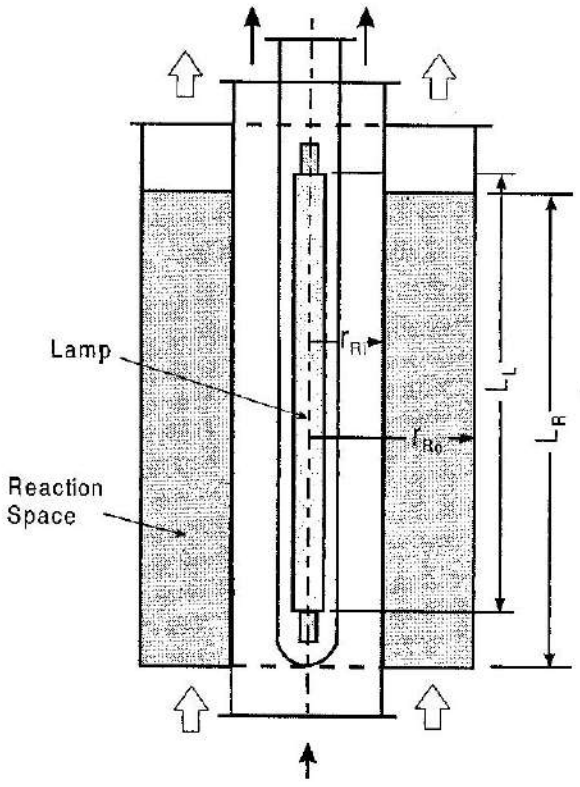

Fig. 1.Geometry of the continuous flow, annular photoreactor. Adapted from [Cassano et al., 1995].

In this equation, $1 \leq g \leq r_{R0}/r_{Ri} = 1/\chi$ and $0 \leq V \leq 1$ provide the definition of the reacting region for the radial and the axial position respectively. The inlet condition is:

$$\Psi_i(0, \gamma) = \Psi_{i,0} \tag{4}$$

This condition states that every reactant enters the reactor with a uniform inlet concentration. Obviously, for products its value is trivially and identically equal to zero. For the stable species, the boundary conditions are:

$$\frac{\partial \Psi_i}{\partial \gamma}(\varsigma, 1) = 0 \tag{5}$$

$$\frac{\partial \Psi_i}{\partial \gamma}(\varsigma, 1/\chi) = 0 \tag{6}$$

Meaning that at the non-permeable reactor walls mass fluxes are zero.

For all but zero and first order reactions this equation must be solved numerically. Central finite difference techniques have been usually employed.

The plug flow reactor

Under fully developed turbulent flow regime the following approximations can be used: (i) the velocity profile is flat and equal to the average velocity and (ii) there is perfect mixing in the radial direction. When this is the case and the reactor walls are not permeable, concentration gradients in the radial direction can be neglected and Eqs. (3), (4), (5) and (6) reduce to:

$$\frac{d\langle \Psi_i(\varsigma, \gamma)\rangle_{A_{R,C}}}{d\varsigma} = \langle \Omega_i(\varsigma, \gamma)\rangle_{A_{R,C}} \tag{7}$$

$A_{R,C}$ indicates an average over the reactor cross section area. The initial condition is:

$$\langle \Psi_i(\varsigma = 0)\rangle_{A_{R,C}} = \Psi_{i,0} \tag{8}$$

It should be specially noted that average values of reaction rates are needed because under no circumstances photons can be very well mixed; consequently, since the photon concentration is normally non-uniform, usually, the reaction rate will be a strong function of the radial position.

III.1.2. *The isothermal, constant volume, well stirred batch reactor* (Fig. 2)

Eq. (1) can be simplified if, due to good mixing conditions, temperature and concentrations are uniform. Then, after integration in the liquid volume the divergence of the mass fluxes can be set identically equal to zero. Since spatial variations in concentrations do not exist, the partial derivative with respect to time becomes an ordinary derivative:

$$\frac{dC_i(t)}{dt} = \langle R_{Hom,i}(\underline{x}, t)\rangle_{V_R} \tag{9}$$

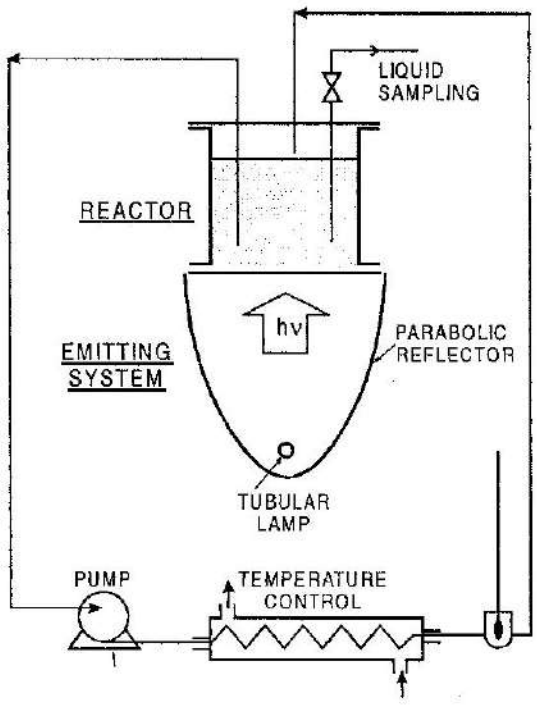

Fig. 2. Schematic diagram of the isothermal, constant volume, well stirred batch reactor.

Note that the reaction rate is still a function of position because the radiation field, always included in the reaction rate, is usually not uniform. Hence:

$$\left\langle \frac{dC_i(\underline{x},t)}{dt} \right\rangle_{V_R} = \frac{d\left\langle C_i(\underline{x},t)\right\rangle_{V_R}}{dt} =$$

$$= \underbrace{\frac{dC_i(t)}{dt}}_{\text{Well mixed reactor}} = \left\langle \underbrace{R_{Hom,i}(\underline{x},t)}_{\text{Radiation field is not uniform}} \right\rangle_{V_R} \qquad (10)$$

With

$$\left\langle R_{Hom,i}(\underline{x},t)\right\rangle_{V_R} = \frac{1}{V_R}\int_{V_R} R_{Hom,i}(\underline{x},t)dV \qquad (11)$$

Even in well-mixed photochemical reactors, the volume average of the reaction rate must be always calculated because usual experimental measurements never represent local values. As it will be seen further ahead, this average operation is important when a reaction rate derived from a reaction scheme (or mechanism) is used to model $R_{Hom,i}$.

Note that the volume of connecting lines in Figure 2 has been considered negligible. This stirring mechanism is suggested for laboratory reactors to avoid the effects produced by the presence of a stirrer inside the reactor thus producing a distortion of the radiation field inside the reaction space.

III.1.3. *The isothermal, batch reactor with recycle* (Fig. 3)

These systems are normally used when the reaction rate is rather slow and single pass operation is not effective. Under the following assumptions: (i) differential operation in V_R (slow reaction and very high recirculation flow rate) and (ii) very good mixing conditions in V_{Tk} we can treat the whole system ($V = V_R + V_{Tk}$) as a well-mixed

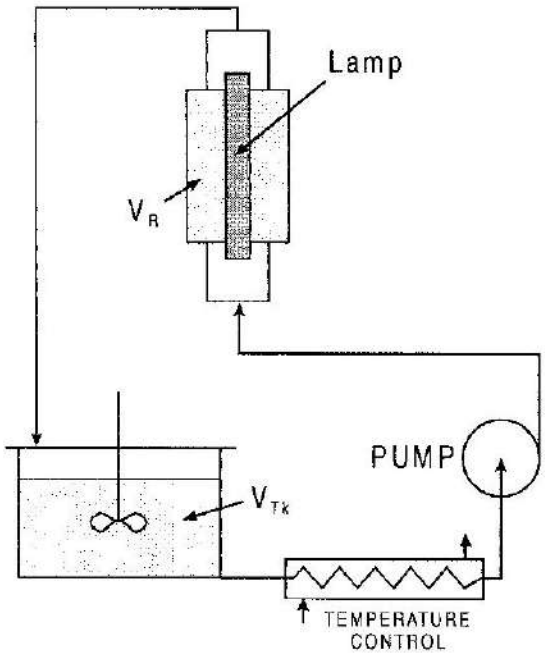

Fig. 3. Schematic diagram of the isothermal, batch reactor with recycle.

batch reactor. Then, since $\underline{\nabla} \cdot \underline{N}_i = 0$ (no concentration gradients, no inlets and outlets), integrating Eq. (1) in the total volume we get:

$$(V_R + V_{Tk})\overbrace{\frac{\left\langle dC_i(\underline{x},t)\right\rangle_V}{dt}}^{\text{Unknown}} =$$

$$= \left\langle R_{Hom,i}(\underline{x},t)\right\rangle_{V_R} V_R + \underbrace{\left\langle R_{Hom,i}(\underline{x},t)\right\rangle_{V_{Tk}} V_{Tk}}_{0} \qquad (12)$$

Note that $R_{Hom,i} \neq 0$ only in V_R, because in V_{Tk} there is no reaction. The average concentration can be divided in two parts:

$$\left\langle C_i(\underline{x},t)\right\rangle_V =$$

$$= \frac{V_R}{V}\underbrace{\left\langle C_i(\underline{x},t)\right\rangle_{V_R}}_{\text{Average on the reactor}} + \frac{V_{Tk}}{V}\underbrace{\left\langle C_i(\underline{x},t)\right\rangle_{V_{Tk}}}_{\text{Average on the tank}} \qquad (13)$$

$$\frac{V_R}{V}\underbrace{\frac{d\langle C_i(\underline{x},t)\rangle_{V_R}}{dt}}_{\text{In the reactor}}+\frac{V_{Tk}}{V}\underbrace{\frac{dC_i}{dt}}_{\text{In the tank}}=$$

$$=\frac{V_R}{V}\underbrace{\langle R_{Hom,i}(\underline{x},t)\rangle_{V_R}}_{\text{Only in the reactor}} \qquad (14)$$

Since $V_R / V < 1$ and the conversion per pass in the reactor is very small, the first term in Eq. (14) is negligible. Then, changes in concentration with time described by Eq. (14) can be measured directly in the tank. The final equation can be written as:

$$\left.\frac{dC_i(t)}{dt}\right]_{Tk}=\frac{V_R}{V_{Tk}}\langle R_{Hom,i}(\underline{x},t)\rangle_{V_R} \qquad (15)$$

A more detailed derivation can be found in [Martín *et al.*, 1996].

III.1.4. *Heterogeneous reactions*

Components of water or air pollution are usually in a fluid phase. Hence we may write equations such as (3), (7), (9) and (15) for the fluid. The fluid may have non-permeable boundaries (the reactor walls) and permeable boundaries (entrances and exits of the system as well as catalytic surfaces where mass fluxes must be equal to the superficial reaction rates). Usually, these reaction rates are modeled as pseudo-homogeneous and, moreover, experimental measurements are usually made in the fluid phase.

Heterogeneous reactions are the result of a process that occurs at phase interfaces. The mass conservation equation has been written for a region in a single phase (the fluid phase, for example). This means that for the differential equation that is only valid for the fluid phase, heterogeneous reactions (surface reactions for example) are just boundary conditions for such differential equation. The problem is very simple to formulate: at steady state and at the boundary of an active surface, the normal mass or molar fluxes must be made equal to the heterogeneous, superficial reaction rate. Then:

$$\text{At } \underline{x} \text{ on the surface} \rightarrow \underbrace{\underline{N}_i\cdot\underline{n}}_{\text{Mass fluxes}}=$$

$$=\underbrace{R_{Het,i}\left(C_i^{surface},T,etc\right)}_{\text{Surface reaction}}=R_{Het,i}(\underline{x},t) \qquad (16)$$

Note that $\underline{n}$ is the outwardly directed normal coming out from the surface, i.e., the flux normal to the surface is equated to the superficial chemical reaction. Typical examples are solid catalyzed reactions or wall reactions occurring in free radical chemistry. Usually reacting surfaces are covered by a boundary layer of the fluid. Then, it is of no surprise that the fluxes be expressed in term of the **diffusive fluxes** exclusively. In any mass balance, we usually have mass fluxes expressed in terms of $\underline{\nabla}\cdot\underline{N}_i$. From standard definitions [Bird *et al.*, 2002, p. 537]:

$$\underbrace{\underline{\nabla}\cdot\underline{N}_i(\underline{x},t)}_{\text{Mass fluxes}}=\underline{\nabla}\cdot\left[\underbrace{\underline{J}_i(\underline{x},t)}_{\text{Diffusional fluxes}}+\underbrace{C_i(\underline{x},t)\,\underline{v}(\underline{x},t)}_{\text{Convective fluxes}}\right]$$

(17)

At the catalytic surfaces, convective fluxes are zero. Diffusional fluxes are zero only at the non permeable walls. Then, when heterogeneous reactions are present at the catalytic surfaces $\underline{\nabla}\cdot\underline{N}_i \neq 0$ even if the reactor is well mixed. Hence, the diffusional fluxes can be made equal to the heterogeneous (superficial) reaction rate:

$$\underbrace{\underline{J}_i(\underline{x},t)\cdot\underline{n}}_{\substack{\text{Normal component of}\\ \text{the diffusional flux}}}=R_{Het,i}(\underline{x},t)\,[=]\,\frac{\text{mole}}{\text{cm}^2\,\text{s}} \qquad (18)$$

Since we are interested in pseudo-homogeneous reaction rates:

$$R_{Hom,i}^{Pseudo}=a_V\,R_{Het,i}=C_{mp}S_g\,R_{Het,i}\,[=]\,\frac{\text{mole}}{\text{cm}^3\,\text{s}}$$

(19)

A typical application can be found in [Cabrera *et al.*, 1997 (b)].

III.2. *Thermal energy conservation equations*

Including heating effects due to radiative transfer and neglecting: (i) energy fluxes due to the diffusion-thermo effect (the Dufour effect), (ii) energy fluxes caused by interdiffusion of the different chemical species, (iii) heat effects produced by viscous dissipation (friction), (iv) heat effects resulting from pressure gradients, (v) heat conduction in the axial direction compared with the convective flow in the same direction and assuming: (vi) constant physical and transport properties and (vii) steady state conditions, the balance of thermal energy for multicomponent systems in cylindrical coordinates is [Bird *et al.*, 2002, ps. 589, 848]:

$$\underbrace{\rho_{mix}\hat{C}_P\left(v_z\frac{\partial T}{dz}\right)}_{\text{Thermal flow in the axial direction}} = \underbrace{k_c\left[\frac{1}{r}\frac{\partial}{\partial r}\left(r\frac{\partial T}{\partial r}\right)\right]}_{\text{Heat conduction in the radial direction}} + \underbrace{\rho Q^{Ext}}_{\text{Radiation heats ources}} - \underbrace{\sum_j \overline{H}_j\left(R_{Hom,i}\right)}_{\text{Enthalpy changes due to chemical reaction}} \qquad (20)$$

Q^{Ext} is an scalar that includes all forms of heating effects produced by energy transmission without contact, i.e., from external bodies (typically, radiation, electrical heating, etc.). In the vast majority of photochemical reactions (employing visible and UV light), heating effects produced by radiation should not be important. However, with lamps emitting significant energy in the infrared region, if the IR radiation is not filtered (i.e., absorbed by cooling devices before entering the reactor), the Q^{Ext} term must be taken into account. In Eq. (20) $\overline{H}_i$ are the partial molar enthalpies of reactants and products. Neglecting heating effects due to radiation, this equation can be re-written in the most familiar form:

$$\rho_{mix}\hat{C}_P\left(v_z\frac{\partial T}{\partial z}\right) = k_c\left[\frac{1}{r}\frac{\partial}{\partial r}\left(r\frac{\partial T}{\partial r}\right)\right] - \underbrace{\sum_j \Delta H_j R_{Hom,j}(\underline{x}, t)}_{\text{Heat of reaction}} \qquad (21)$$

In Eq. (18) the index j stands for the j different chemical reactions occurring in the system. k_c is the thermal conductivity. We can now change the scales for making Eq. (21) dimensionless:

$$\tau = \frac{T - T_0}{T_0 - T_c}, \quad Pe_T = \frac{\rho_{mix}\hat{C}_P\langle v_z\rangle}{k_c},$$

$$Q_R = \frac{L_R\left(\sum_j -\Delta H_j R_j\right)}{\rho_{mix}\hat{C}_P\langle v_z\rangle(T_0 - T_c)}$$

T_0 is the inlet temperature and T_C some fixed temperature in the system, for example that of the refrigerating water that for simplicity is assumed constant. Note that temperatures are made dimensionless in such a way that they will take on values of 0 at the reactor entrances ($T = T_0$). The boundary conditions for the reactor walls are written in terms of the Newton equation for cooling: $[(q)_{radial} = h\,(T - T_c)]$. h is the film heat transfer coefficient. This adoption also permits for exothermic reactions to have (To – Tc) > 0 always. Pe_T is the Peclet number for radial heat transport. The dimensionless thermal energy equation is then:

$$\underbrace{U_x(\gamma)\frac{\partial\tau(\gamma,\varsigma)}{\partial\varsigma}}_{\text{Axial thermal flow}} - \underbrace{\frac{1}{Ge\,Pe}\left[\frac{1}{\lambda}\frac{\partial}{\partial\lambda}\left(\gamma\frac{\partial\tau(\gamma,\varsigma)}{\partial\gamma}\right)\right]}_{\text{Heat conduction in the radial direction}} = \underbrace{Q_R(\gamma,\varsigma)}_{\text{Heat of reaction}} \qquad (22)$$

The inlet condition is:

$$\tau(0, \gamma) = 0 \qquad (23)$$

stating that the fluid enters the reactor with uniform temperature. The boundary

conditions that take into account heat transfer from the reactor walls into the cooling liquid are:

$$\frac{\partial\tau(\varsigma,1)}{\partial\gamma} = Nu_i(\tau-1) \qquad (24)$$

$$\frac{\partial\tau(\varsigma,1/\chi)}{\partial\gamma} = -Nu_o(\tau-1) \qquad (25)$$

Nu is the Nusselt number [$Nu_o = hr_{Ro}/k_c$, $Nu_i = hr_{Ri}/k_c$] that involves the thermal conductivity of the fluid and the film heat transfer coefficient of the refrigerating liquid. If the reactor operates under almost isothermal conditions Eqs. (22) to (25) are not needed.

Under plug flow conditions let us integrate Eq. (22) over the cross sectional area of the tubular reactor:

$$\int_{A_{R,C}} U_z(\gamma)\frac{\partial\tau(\gamma,\varsigma)}{\partial\varsigma}\,dA -$$

$$-\int_{A_{R,C}} \frac{1}{Ge\,Pe_T}\left[\frac{1}{\gamma}\frac{\partial}{\partial\gamma}\left(\gamma\frac{\partial\tau(\gamma,\varsigma)}{\partial\gamma}\right)\right]dA = \int_{A_{R,C}} Q_R(\gamma,\varsigma)\,dA \qquad (26)$$

$$\frac{d}{d\varsigma}\int_{A_{R,C}} U_z(\gamma)\tau\,d\beta\,\gamma\,d\gamma -$$

$$-\frac{1}{Ge\,Pe_T}\int_{A_{R,C}}\left[\frac{1}{\gamma}\frac{\partial}{\partial\gamma}\left(\gamma\frac{\partial\tau}{\partial\gamma}\right)\right]d\beta\,\gamma\,d\gamma = \int_{A_{R,C}} Q_R\,d\beta\,\gamma\,d\gamma \qquad (27)$$

A mixed cup dimensionless average temperature and a reactor cross section average heat of reaction can be defined:

$$\langle U_z\rangle_{A_{R,C}}\left[\frac{\pi(1-\chi^2)}{\chi^2}\right]\langle\tau\rangle_{A_{R,C}} = \int_{A_{R,C}}\tau U_z\,d\beta\,\gamma\,d\gamma$$

$$\left[\frac{\pi(1-\chi^2)}{\chi^2}\right]\langle Q_R\rangle_{A_{R,C}} = \int_{A_{R,C}} Q_R\,d\beta\,\gamma\,d\gamma \qquad (28)$$

Then:

$$\langle U_z\rangle_{A_{R,C}}\left[\frac{\pi(1-\chi^2)}{\chi^2}\right]\frac{d\langle\tau\rangle_{A_{R,C}}}{d\varsigma} +$$

$$+\frac{2\pi}{Ge\,Pe_T}\left[\left.\frac{\partial\tau}{\partial\gamma}\right|_{\gamma_i} - \gamma_o\left.\frac{\partial\tau}{\partial\gamma}\right|_{\gamma_o}\right] =$$

$$=\left[\frac{\pi(1-\chi^2)}{\chi^2}\right]\langle Q_R\rangle_{A_{R,C}} \qquad (29)$$

Applying boundary conditions (24) and (25) and assuming that $Nu_o = Nu_i = Nu$:

$$\langle U_z\rangle_{A_{R,C}}\frac{d\langle\tau\rangle_{A_{R,C}}}{d\varsigma} + \frac{Nu}{Ge\,Pe_T}\frac{2(1+\chi)\chi}{(1-\chi^2)}(\tau-1) =$$

$$=\langle Q_R\rangle_{A_{R,C}} \qquad (30)$$

Since the exchange surface area per unit reactor volume is:

$$\frac{2\pi(1+\chi)\chi}{\pi(1-\chi^2)r_{Ri}} = a_V\,[=]\,\frac{cm^2}{cm^3} \qquad (31)$$

We finally have:

$$\langle U_z(\gamma)\rangle_{A_{R,C}}\frac{d\langle\tau(\gamma,\varsigma)\rangle_{A_{R,C}}}{d\varsigma} +$$

$$+\underbrace{\frac{Nu\,a_V\,r_{Ri}}{Ge\,Pe_T}(\tau-1)}_{\text{Heat removal}} = \underbrace{\langle Q_R(\gamma,\varsigma)\rangle_{A_{R,C}}}_{\text{Heat produced}} \qquad (32)$$

Eq. (32) permits to calculate temperature profiles along the axial direction in a plug flow reactor.

IV. Radiation transport

When writing the rate of a photochemical reaction it is necessary to make the distinction between dark and radiation

activated (lighted) steps. To treat the dark reactions one uses the same methodology as for conventional reactors; the main difference appears when evaluating the rate of the radiation-activated step. The existence of this very particular step constitutes the main distinctive aspect (and the most important one) between thermal (or thermal catalytic) and radiation activated reactions.

The rate of the radiation-activated step is directly proportional to the absorbed, useful energy through a property that has been defined as the **Local Volumetric Rate of Photon Absorption.** The L.V.R.P.A, (e^a_λ), represents the amount of photons that are absorbed per unit time and unit reaction volume. The L.V.R.P.A depends on the radiation field (photon distribution) existing in the reaction space; hence, we must know the radiation field within the photoreactor. This radiant energy distribution is not uniform in space due to several causes; among them, the attenuation produced by the species absorption is always present. Additional phenomena, usually also important, are the physical properties and geometrical characteristics of the lamp-reactor system. The value of the L.V.R.P.A. is defined for monochromatic radiation but it can be extended to polychromatic fields by performing integration over all useful wavelengths. Useful wavelength range is defined by the overlapping ranges of lamp emission, reactor wall transmission, reactant or catalyst absorption and, eventually, reflector reflectance.

The general structure for calculating the rate of the activation step may be described as it is schematically indicated in Figure 4. As it was shown before, the mass balances ask for expressions formulating the reaction rates; be it a molecular or a free radical reaction mechanism, always some of the steps (generally one) are initiated by radiation absorption. The radiation activated step kinetics is always written in terms of (e^a_λ). The evaluation of the L.V.R.P.A. is performed stating first the general radiation transport equation that requires the appropriate constitutive equations for absorption, emission and scattering. The resulting radiative transfer equation is then successively applied to the reaction space where there is only absorption (in homogeneous media) or absorption and scattering (in heterogeneous media), and to the lamp where emission is the prevailing phenomenon. Combining both results one can obtain, in a straightforward manner, the local value of the rate of radiation absorption. With this information the rate equation is developed and incorporated into the mass balance.

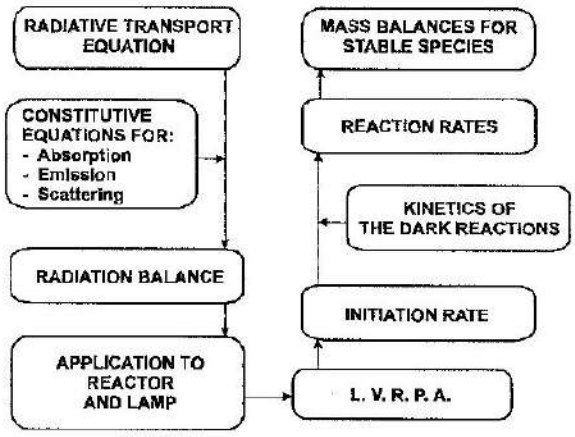

Fig. 4. Evaluation of the rate of the initiation step. Adapted from [Cassano et al., 1995].

IV.1. *Spectral Specific Intensity*

Under usual conditions, propagation of photons may be represented by bundles of rays with a given energy. These rays may be specified by the **Spectral Specific Intensity** that is the fundamental property for characterizing radiation fields. In Figure 5, let dA be an arbitrarily oriented small area about the space coordinate $\underline{x}$, P a point in this area and $\underline{n}$ be the normal to the area at point P. At a given time there will be radiation rays associated with this surface element that may be traveling with different directions. Energy may be transmitted through, emitted by or reflected on this elementary surface. Let us consider a specific direction along which we draw a

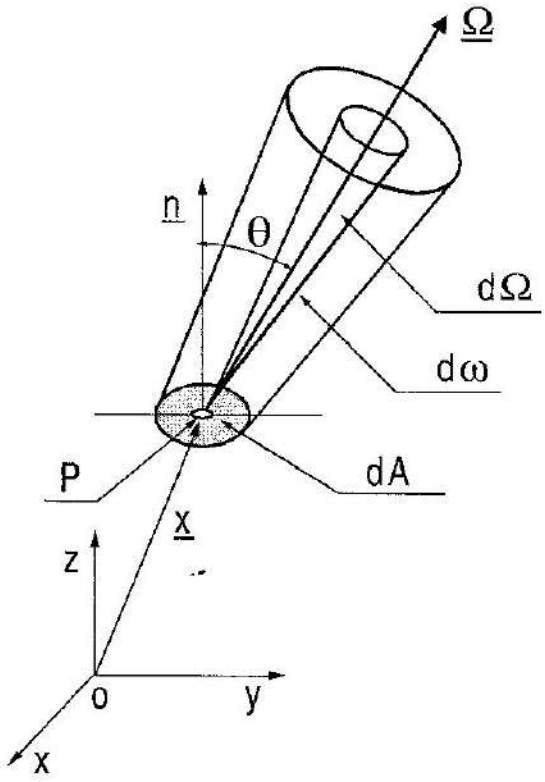

Fig. 5. Characterization of the spectral specific intensity. Adapted from [Cassano et al., 1995].

line that is characterized by the unit direction vector $\underline{\Omega}$ that makes an angle θ to the normal $\underline{n}$.The vector $\underline{\Omega}$ coincides with the axis of an elementary cone of solid angle $d\Omega$. All elementary solid angles corresponding to rays parallel to the direction $\underline{\Omega}$ passing through dA define a truncated semi-infinite cone $d\omega$, whose cross sectional area perpendicular to $\underline{\Omega}$ at the point P will be dA $\cos\theta$. Let dE_λ be the total amount of radiative energy passing through the area dA inside the cone $d\omega$ in the time dt and with an energy in the wavelength range between λ and $\lambda + d\lambda$. The spectral specific intensity is defined as:

$$I_\lambda(\underline{x},\underline{\Omega},\underline{t},\underline{\lambda}) = \lim_{dA,d\Omega,dt,d\lambda\to 0}\left(\frac{dE_\lambda}{dA\cos\theta\, d\Omega\, dt\, d\lambda}\right) \qquad (33)$$

According to Eq. (33) the Spectral (monochromatic) Specific Intensity is the amount of radiative energy streaming through a unit area perpendicular to the direction of propagation $\underline{\Omega}$, per unit solid angle Ω about the direction $\underline{\Omega}$, per unit wavelength about the wavelength λ, and per unit time t. In photoreactor engineering, the usual units for I_λ are einstein (or joule) per square meter (or square cm), per steradian, per unit wavelength interval (or unit frequency interval) and per second.

Quantum theory introduces the proportionality between frequency and energy. The energy of a quantum is $e = h\nu = hc/\lambda \cdot h = 6.626 \times 10^{-27}$ erg s, is the Plank's constant. c is the speed of light (2.9979×10^{10} cm/s) and λ is the wavelength in cm. To some extent, a quantum is a unit of energy, but its magnitude is not fixed because it varies with the wavelength (or the frequency). The best definition of a quantum is to say that is the radiant energy equal to hν. Whatever it is, when one molecule or an atom absorbs one quantum, a change in that molecule or atom from one level of energy to another will be produced; i.e., its energy will have been increased by an amount equal to one quantum. Similarly, if one mole absorb one quanta, the energy absorbed is $N\,h\,c/\lambda$, where $N = 6.023 \times 10^{23}$ molecules/gmole is the Avogadro's number. Hence the energy of a gram mole of a given material will be increased by $N\,h\,c/\lambda$. The quantity of radiant energy equal to $N\,h\,c/\lambda$ is called **one einstein**. All units in J (or W) can be converted into einstein (or einstein/s) with the proper transformation. This new unit is very convenient in photochemistry because the photochemical activation is the result of the interaction of one molecule with one photon having one quantum of energy or, in other terms, one mole with one mole of photons that have energy equal to one einstein. The transformation can be obtained as follows:

$$I_\lambda^{eins} = \frac{\lambda}{N h c} I_\lambda^{W}, \text{ wit } I_\lambda^{eins}[=]\frac{\text{einstein}}{\text{s cm}^2\text{ sr}}$$

$$\text{and } I_\lambda^{W}[=]\frac{\text{W}}{\text{cm}^2\text{ sr}} \text{ (both monochromatic).}$$

Then, the conversion constant is

$$k_{w\to eins} = \frac{1}{N\,h\,c} = 8.358 \times 10^{-9}\ \frac{\text{einstein/s}}{\text{W nm}}$$ and:

$$1\ \text{Einstein} = \frac{0.11964}{\lambda(\text{m})}\ \text{Ws}.$$

IV.2. *Homogeneous media*

From the radiation viewpoint a homogeneous medium means that scattering does not need to be considered. This is a great simplification for modeling and design. In this case, the intensity of a monochromatic beam of radiation in any arbitrary direction $\underline{\Omega}$ will be changed only by emission or absorption. Emission can be usually neglected particularly for low temperature processes. Then, at any point in space $\underline{x}$ and any time t, we are left with the three dimensional form of the Bouguer-Lambert "law» for monochromatic radiation absorption in homogeneous media:

$$\frac{dI_{\lambda,\underline{\Omega}}(\underline{x},t)}{ds} + \kappa_\lambda(\underline{x},t)\, I_{\lambda,\underline{\Omega}}(\underline{x},t) = 0 \qquad (34)$$

In Eq. (34) s is measured along a direction in space ($\underline{\Omega}$) for photons transport. With the following simplifications: (i) the absorption coefficient bears a linear relationship with the concentration of the absorbing species and (ii) the radiation beam is unidirectional (usually a collimated beam of parallel rays), Eq. (34) reduces to the well-known Lambert-Beer equation used in spectroscopy. The spectral specific intensity must not be confused with radiation fluxes. They are equal only for unidirectional irradiation, a case very distant from the general one. Note that even under steady illumination, intensities may change with time because so may do the absorption coefficient.

In the most general case, radiation may be arriving at one point inside a photochemical reactor from all directions in space. For a photochemical reaction to occur this radiation must be absorbed by an elementary reacting volume (a material point in space); thus, pencils of radiation coming from all directions must cross the whole elementary surface that bounds such an element of volume. Consequently, the important photochemical property is the **Spectral Incident Radiation** given by:

$$G_\lambda(\underline{x},t) = \int_{\underline{\Omega}} I_{\underline{\Omega},\lambda}(\underline{x}.\,t)\, d\Omega \qquad (35)$$

In Eq. (35) integration for all possible directions $\underline{\Omega}$ over the entire spherical space has been performed. In a spherical coordinate system located at the point of incidence (the reacting elementary volume), since $d\Omega = \sin\theta d\phi d\theta$, the arriving incident radiation is:

$$G_\lambda(\underline{x},t) = \int_{\theta_1}^{\theta_2}\int_{\phi_1}^{\phi_2} I_{\theta,\phi,\lambda}(\underline{x},t)\,\sin\theta\, d\phi\, d\theta \qquad (36)$$

$[\theta_1, \theta_2]$ and $[\phi_1, \phi_2]$ are the integration limits that define the space from which radiation arrives at the point of incidence. If radiation energy arrives from the whole 4π space, then the limits for θ extend from 0 to π and those for ϕ extend from 0 to 2π. For each point of incidence, in practice, these limits are defined by the extension of the lamp.

For polychromatic radiation, integration over the wavelength range of interest must be performed (accounting for the overlapping wavelength regions of lamp emission, reactor wall transmission and radiation absorbing species absorption coefficient):

$$G_{\Sigma\lambda}(\underline{x},t) = \int_{\lambda_1}^{\lambda_2}\int_{\theta_1}^{\theta_2}\int_{\phi_1}^{\phi_2} I_{0,\phi,\lambda}(\underline{x},t)\,\sin\theta\, d\phi\, d\theta\, d\lambda \qquad (37)$$

In the elementary volume of radiation absorption, for single photon absorption, energy is absorbed according to:

$$e^a_\lambda(\underline{x},t) = \kappa_\lambda(\underline{x},t)\, G_\lambda(\underline{x},t) \qquad (38)$$

e^a_λ is the **Spectral** (monochromatic) **Local Volumetric Rate of Photon Absorption** (L.V.R.P.A.) or the spectral rate of photon

absorption per unit reaction volume, very often improperly called «Absorbed Intensity». Its units are einstein per cubic meter and per second, very different from those corresponding to an Intensity. κ is the absorption coefficient that is always some function of the concentration of the absorbing species. The well-known Beer's approximation can be used for homogeneous, dilute systems. Note that since G is a function of position, so is e^a_λ. G may be a function of time for lamps operating under unsteady state conditions. The absorption coefficient may be a function of position for reactors operating under strong concentration gradients and a function of time for systems where absorption changes with the reaction progress (the reactant absorbs radiation, some reaction products absorb radiation, etc.) or when using a photocatalyst the solid semiconductor is not stable in its optical properties. For polychromatic radiation:

$$e^a_{\Sigma\lambda}(\underline{x},t) = \int_{\lambda_1}^{\lambda_2}\int_{\theta_1}^{\theta_2}\int_{\phi_1}^{\phi_2} \kappa_\lambda I_{\theta,\phi,\lambda}(\underline{x},t)\,\sin\theta\,d\phi\,d\theta\,d\lambda \quad (39)$$

Thus, to evaluate the L.V.R.P.A. we must know the Spectral Specific Intensity at each point inside the reactor. Its value can be obtained from the photon transport equation.

IV.3. *Heterogeneous media*

In more general terms, the radiative transfer equation may be rationalized considering a balance of monochromatic photons along a given direction of radiation propagation:

Time rate of change of $\underline{\Omega}$, λ photons in the volume V	+	Net flux of $\underline{\Omega}$, λ photons leaving the volume V across its bounding surface A	=	Net gain (loss) of $\underline{\Omega}$, λ photons owing to emission, absorption, in- and out-scattering in the volume V

$$\frac{\partial}{\partial t}\int_V \mathcal{N}_{\underline{\Omega},\lambda}\,dV + \int_A \mathcal{N}_{\underline{\Omega},\lambda}\,(c\underline{\Omega})\cdot\underline{n}\,dA =$$

$$= -\int_V \mathcal{N}^a_{\underline{\Omega},\lambda}\,dV + \int_V \mathcal{N}^e_{\underline{\Omega},\lambda}\,dV +$$

$$+ \int_V \mathcal{N}^{s-in}_{\underline{\Omega},\lambda}\,dV - \int_V \mathcal{N}^{s-out}_{\underline{\Omega},\lambda}\,dV$$

Transforming the area integral into a volume integral (with the Divergence theorem) all the terms will have the same integration limits. Then, multiplying by (hν) and considering that $I_\lambda = ch\nu\,(\mathcal{N}_{\lambda,\Omega})$ we can extract the differential equation in terms of Specific Intensities. In symbolic form [Ozisik, 1973, p 251]:

$$\frac{1}{c}\frac{\partial I_{\underline{\Omega},\lambda}}{\partial t} + \underline{\nabla}\cdot\left(I_{\underline{\Omega},\lambda}\,\underline{\Omega}\right) =$$

$$- W^a_{\underline{\Omega},\lambda} + W^e_{\underline{\Omega},\lambda} + W^{s-in}_{\underline{\Omega},\lambda} - W^{s-out}_{\underline{\Omega},\lambda} \quad (40)$$

Eq. (40) is the general form of the radiation conservation equation for $\underline{\Omega},\lambda$ photons. Usually the first term can be neglected (the factor 1/c makes it always very small); i.e., at a given time the radiation field reaches its steady state almost instantaneously. However $I_{\underline{\Omega},\lambda}$ will change with time if the boundary condition associated with Eq. (40) is time dependent (for example, in a photoreactor having a time dependent radiation source emission; typically, a solar reactor) or if the state variables which appear in the constitutive equations for any one of the different processes $W^a_{\underline{\Omega},\lambda}$, $W^e_{\underline{\Omega},\lambda}$, $W^{s-in}_{\underline{\Omega},\lambda}$ and $W^{s-out}_{\underline{\Omega},\lambda}$, change with time.

Absorption and out-scattering are modeled in the same way that absorption is accounted for in homogeneous systems. Emission should be modeled according to the particular involved process. However, as said before, in most photochemical reactions it can be usually neglected.

In-scattering is responsible for most of the complications that arise when scattering of radiation is an important phenom-

enon. It results from the almost unavoidable existence of multiple scattering. When scattering is not single, a photon scattered out from one direction may interact with other particles. Then, part of the radiation that is scattered in space may be incorporated to the stream of $\underline{\Omega}$, λ photons according to the scattering distribution function (the phase function). This process may occur from all directions in space and for all wavelengths. Thus, ($\underline{\Omega}$, λ'), ($\underline{\Omega}'$, λ) and ($\underline{\Omega}'$, λ') photons may be incorporated to the family of $\underline{\Omega}$, λ photons. The contribution must be computed for all possible directions and wavelengths. When radiation is arriving to the volume element from all directions and all wavelengths, this integration yields [Ozisik, 1973, p. 27]:

$$W_{\underline{\Omega},\lambda}^{s-in} = \frac{1}{4\pi} \int_{\Omega'=4\pi} \int_{\lambda'=0}^{\lambda'=\infty} \sigma_\lambda(\underline{x}, t) \times$$

$$p(\lambda' \to \lambda, \underline{\Omega}' \to \underline{\Omega}) I_{\underline{\Omega}',\lambda'}(\underline{x}, t) d\lambda' d\Omega' \qquad (41)$$

where p is the phase function. The above equation is valid for incoherent scattering. The scattering is incoherent or anelastic when the frequency of the scattered radiation is different from that corresponding to the incident radiation; i.e., the radiation beam changes its energy. Otherwise the scattering is elastic or coherent. For coherent scattering:

$$W_{\underline{\Omega},\lambda}^{s-in} = \frac{1}{4\pi} \int_{\underline{\Omega}'=4\pi} \sigma_\lambda(\underline{x}, t)\, p(\underline{\Omega}' \to \underline{\Omega}) I_{\underline{\Omega}',\lambda}(\underline{x}, t)\, d\Omega' \qquad (42)$$

With the normalizing condition:

$$\frac{1}{4\pi} \int_{\underline{\Omega}'=4\pi} p(\underline{\Omega}' \to \underline{\Omega})\, d\Omega' = 1 \qquad (43)$$

Scattering is isotropic when p = 1. Isotropic scattering requires, among other requirements, that at least the scattering material be homogeneous and isotropic, and that the surrounding medium be also isotropic. More details on phase functions can be found in the classical references of [van de Hulst, 1957; Ozisik, 1973; Siegel and Howell, 1992].

Very often the sum of the absorption coefficient and the scattering coefficient is called the **extinction coefficient**:

$$\beta_\lambda(\underline{x}, t) = \kappa_\lambda(\underline{x}, t) + \sigma_\lambda(\underline{x}, t) \qquad (44)$$

The extinction coefficient is usually used together with the **scattering albedo** that is defined as:

$$\omega_\lambda(\underline{x}, t) = \frac{\sigma_\lambda(\underline{x}, t)}{\beta_\lambda(\underline{x}, t)} \qquad (45)$$

Working photon transport equation

Going back to Eq. (40) one can neglect the transient term and substitute the different constitutive relationships. After defining a directional coordinate s along the ray path, from elementary calculus it is known that:

$$\underline{\nabla} \cdot (\underline{\Omega}\, I_{\underline{\Omega},\lambda}) = \underline{\Omega} \cdot \underline{\nabla} I_{\underline{\Omega},\lambda} = \frac{1}{|\underline{\Omega}|} \frac{dI_{\underline{\Omega},\lambda}}{ds} = \frac{dI_{\underline{\Omega},\lambda}}{ds} \qquad (46)$$

because the unit vector $\underline{\Omega}$ is independent of position. The last term in Eq. (46) is the directional derivative of the intensity along the direction defined by the unit vector Ω. Then, the following working photon transport equation for coherent scattering is obtained:

$$\frac{dI_{\underline{\Omega},t}(s, t)}{ds} + \underbrace{\kappa_\lambda(s, t) I_{\underline{\Omega},t}(s, t)}_{\text{Absorption}} +$$

$$+ \underbrace{\sigma_\lambda(s, t) I_{\underline{\Omega},t}(s, t)}_{\text{Out - scattering}} = \underbrace{j_\lambda^e(s, t)}_{\text{Emission}} +$$

$$+ \underbrace{\frac{1}{4\pi} \sigma_\lambda(s, t) \int_{\Omega=4\pi} p(\underline{\Omega}' \to \underline{\Omega})\, I_{\underline{\Omega}',\lambda}(s, t)\, d\Omega'}_{\text{In-scattering}} \qquad (47)$$

There is an important assumption implicit in the derivation of this expression; it may be applied only to a medium that may be considered as pseudo-homogeneous.

This restriction puts some limits to the application of this equation in heterogeneous media. It should have a valid application when the existing heterogeneities are of small size and they are present in small concentrations; let us say particle sizes smaller than 2 mm and concentration of solids below 10 percent. If this is not the case a different approach may be necessary.

This consideration lead us to conclude that under the validity conditions already established for Eq. (47), most likely, also conditions for independent scattering will prevail. Independent scattering means that particles are sufficiently far from each other and that it is possible to study the scattering by one particle without reference to the others. This condition prevails when the clearance between particles is sufficiently large relative to both the particle diameter and radiation wavelength [Siegel and Howell, 1992].

Perhaps one of the most important conclusions that can be drawn from this equation is that in heterogeneous reacting systems classical forms of analyzing the light distribution inside the photochemical cell (i.e., the Lambert-Beer equation) would be incorrect and very likely, useless. This conclusion is particularly important when the effect of the Incident Radiation on solid-fluid photocatalytic reaction rates is investigated. The second conclusion of significance is that, with only a very few exceptions (collimated beams), radiation transport is a three-dimensional phenomenon, and one-dimensional models cannot be always used with confidence.

V. Emission by tubular lamps. The line source with spherical emission (LSSE model)

The simplest, fairly realistic model published in the literature [Jacob and Dranoff, 1966; Cassano *et al.*, 1986] is the LSSE model. The following assumptions are made (Fig. 6):

1. The source is a line with uniform emission along its length (axial direction).

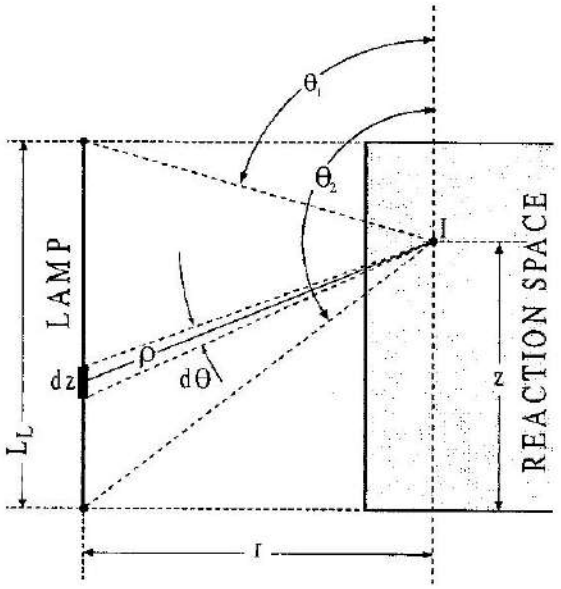

LINEAR LAMP

Fig. 6. The Line Source with Spherical Emission (LSSE) model.

2. The line is considered an infinite succession of ideal point sources, each one emitting in a spherical manner over an angle of 4π.

3. This emission is isotropic (no preferential direction of emission).

For this model we need a special definition of the Specific Intensity because the lamp does not have a defined surface of emission:

$$I_\lambda^* = \frac{dP_\lambda}{dz\, d\Omega\, d\lambda} \qquad (48)$$

In this case: $I_\lambda^* = I_\lambda^*(s,\theta,t)$. Recall that this is not the same definition that is used in radiation field theory for three-dimensional emission produced by real bodies.

If we consider for simplicity a participating, absorbing medium with no scattering, the Radiative Transfer Equation (RTE) is:

$$\frac{dI_\lambda^*(s,\theta,t)}{ds} = -\kappa(s,t)\, I_\lambda^*(s,\theta,t) \qquad (49)$$

According to Figure 6, the boundary condition at the point of radiation entrance to the reactor wall is represented by:

$$I_\lambda^*(s_R, \theta, t) = I_\lambda^{*,0}(t) \qquad (50)$$

One must notice that this Intensity is independent of direction, a condition that is derived from the assumption of isotropic emission by the lamp. For each particular direction, it corresponds to the lamp emission intensity since the medium between the lamp and the reactor wall is usually diactinic.

Emission by the lamp is [Eq. (48)]:

$$dP_{\lambda,L} = I_\lambda^{*,0} dz\, d\Omega\, d\lambda \qquad (51)$$

$$I_\lambda^{*,0} = \frac{P_{\lambda,L}}{\int_0^{4\pi} d\Omega \int_0^{L_L} dz} = \frac{P_{\lambda,L}}{4\pi L_L} \qquad (52)$$

Integrating Eq. (49) and considering Eqs. (50) and (52):

$$I_\lambda^*(s, \theta, t) = \frac{P_{\lambda,L}}{4\pi L_L} \exp\left[- \int_{s=s_R}^{s} \kappa_\lambda(\bar{s}, t) d\bar{s} \right] \qquad (53)$$

The actual output power from a differential element of the lamp must be equal to that described by the LSSE model. Then:

$$dP_\lambda = I_\lambda dA \cos\theta_n\, d\Omega\, d\lambda = I_\lambda^*\, dz\, d\Omega\, d\lambda \qquad (54)$$

And:

$$I_\lambda\, dA \cos\theta_n = I_\lambda^*\, dz \qquad (55)$$

Using Eq. (55) and the definition of the solid angle:

$$d\Omega = \frac{dA \cos\theta_n}{\rho^2} \qquad (56)$$

the following equation is obtained:

$$I_\lambda\, d\Omega = I_\lambda^* \frac{dz}{\rho^2} \qquad (57)$$

With Eq. (57) and the definition of the LVRPA:

$$e_\lambda^a(\underline{x}, t) = \kappa_\lambda(\underline{x}, t) \int_{\Omega_s} I_\lambda d\Omega = \kappa_\lambda(\underline{x}, t) \int_{L_L} I_\lambda^*(s, \theta, t) \frac{dz}{\rho^2} \qquad (58)$$

$\underline{x}$ is a position inside the reactor. It bears a univocal relationship with s, the distance traveled by the radiation bundle. Ω_s is the solid angle defining the extension of the lamp.

Substituting Eq. (53) into Eq. (58):

$$e_\lambda^a(\underline{x}, t) = \frac{P_{\lambda,L}}{4\pi L_L} \kappa_\lambda(\underline{x}, t) \int_0^{L_L} \exp\left[- \int_{s_R}^{s} \kappa_\lambda(\bar{s}, t) d\bar{s} \right] \frac{dz}{\rho^2} \qquad (59)$$

From Figure 6, since:

$$\rho(\theta)\cos\theta = r \quad \text{and} \quad \rho(\theta)\sin\theta = z$$

$$\frac{dz}{\rho^2} = \frac{d\theta}{r} \qquad (60)$$

In this equation r is the radial distance, perpendicular to the lamp axis, measured from the lamp "line" to the point of radiation incidence inside the reactor $\underline{x}$. With this substitution, the LVRPA is:

$$e_\lambda^a(\underline{x}, t) =$$

$$= \frac{P_{\lambda,L}}{4\pi L_L} \kappa_\lambda(\underline{x}, t) \int_{\theta=\theta_1}^{\theta=\theta_2} \frac{d\theta}{r} \exp\left[- \int_{s=s_R}^{s} \kappa_\lambda(\bar{s}, t) d\bar{s} \right] \qquad (61)$$

From plane trigonometry, the new limits of integration, θ_1 and θ_2 are:

$$\theta_1 = \tan^{-1}\left(\frac{r}{L_L - z} \right) \text{ and } \theta_2 = \tan^{-1}\left(\frac{r}{-z} \right) \qquad (62)$$

Eqs. (61) and (62) are normally the working expressions for using the LSSE model. As in any other model, Eq. (61) must incorporate the reactor wall compounded transmission coefficient to account for reflections and internal transmission. Note

that Eq. (61) is valid for homogeneous media because so was the starting equation [Eq. (49)]. Extensions to heterogeneous media is a straightforward procedure.

VI. Homogeneous systems. Application to an annular photoreactor

This application will have two parts: (i) the description of a methodology to obtain an intrinsic kinetics in a batch laboratory reactor, and (ii) the description of the methodology to scale-up results for a tubular, pilot plant reactor.

VI.1. *Reaction kinetics*

A very simple case will be used to illustrate the procedure. For any process employing radiation having a wavelength below 300 nm, direct photolysis is almost unavoidable. Hence, even if in practice an oxidant will always be used (for example, hydrogen peroxide) the parallel photolysis must be also modeled. 2,4-dichlorophenoxyacetic acid (2,4-D) is a widespread herbicide that is known to have a high level of toxicity. Its relatively high solubility in water facilitates its migration to natural courses where it is also known that it may last for several weeks due to its long mean lifetime. The reaction using UV alone with 2,4-D shows most of the features that must be taken into account to model a homogeneous reactor for AOTs. Although it is a rather slow reaction that needs to be complemented with a stronger oxidation, it can be used to illustrate some of the concepts previously developed. As reported by [Cabrera *et al.*, 1997 (a)], kinetic studies were performed in a well-stirred, batch, cylindrical photoreactor irradiated from the bottom (Fig. 2). Monochromatic light (λ = 254 nm) was used. Analyses of the results were performed as it is described in what follows.

VI.1.1 *Radiation Field*

In 1985 [Alfano *et al.*, 1985] studied the above described reactor geometry using a three-dimensional (r, z, β) model. Results were experimentally verified with variable spatial position microreactors [Alfano *et al.*, 1986 (a); Alfano *et al.*, 1986 (b)]. It was found that for **the used geometry and dimensions** radial and angular variations were not very significant. With this background, a one-dimensional model (y-coordinate) can be adopted. Then, Incident Radiation [Eq. (36)] can be described by:

$$G_\lambda(y) = G_{W,\lambda} \exp(-\kappa_{T,\lambda}\, y) \qquad (63)$$

In Eq. (63), $G_{W,\lambda}$ is the Incident radiation at the wall of the reactor bottom (y = 0) and $\kappa_{T,\lambda}$ is the total absorption coefficient of reactant and products. It must be noted that the optical properties of the reacting medium change with the reaction evolution. This is not only due to the decrease in 2,4-D concentration; on the contrary, during part of the course of the reaction, at 253.7 nm, the absorption coefficient of the reacting mixture increases, indicating an important effect due to absorption by the reaction products. Consequently, even in a first approximation, the system must be characterized by **a minimum** of two absorption coefficients: (i) one corresponding to the reactant (2,4-D) and (ii) a different one corresponding to the reacting mixture, being both a function of time. These values, as well as $G_{W,\lambda}$ can be experimentally measured. It should be also noticed that, if desired, the Incident Radiation at y = 0 can be theoretically predicted with great accuracy with [Alfano *et al.*, 1985] radiation model.

The derivation of Eq. (63) needs some careful analysis. First, note that in **any one-dimensional model**, the intensity has the special characteristic that only one component of the three-dimensional representation of the radiation field is different from zero. In general, with the Dirac delta function:

$$I_\lambda(\underline{x}, \underline{\Omega}, t) = \bar{I}(\underline{x}, t)\, \delta\left(\underline{\Omega} - \underline{j}\right) \qquad (64)$$

$$\delta = \begin{cases} \int_0^\infty \delta\left(\hat{\underline{\Omega}} - \underline{j}\right) d\Omega = 1 & \text{for } \hat{\underline{\Omega}} = \underline{j} \\ 0 & \text{for } \hat{\underline{\Omega}} \neq \underline{j} \end{cases} \qquad (65)$$

This equation indicates that radiation transport is permitted only along the direction corresponding to the unit vector in the single direction of radiation propagation "y". Note also that the units for this "special, one-dimensional intensity" are:

$$\bar{I}_\lambda(\underline{x},t)=\bar{I}_\lambda(y,t)[=]\frac{\text{Einstein}}{m^2\,s}\qquad\text{With}$$

$$\delta\left(\underline{\Omega}-\underline{j}\right)[=]\frac{1}{sr}$$

In this case, the Incident Radiation results:

$$G_\lambda(y,t)=\int_\Omega I_\lambda(\underline{x},\underline{\Omega},t)\,d\Omega=$$

$$=\int_\Omega \bar{I}_\lambda(\underline{x},t)\,\delta\left(\underline{\Omega}-\underline{j}\right)d\Omega=$$

$$=\bar{I}_\lambda(y,t)\int_\Omega\delta\left(\underline{\Omega}-\underline{j}\right)d\Omega=\bar{I}_\lambda(y,t)\qquad(66)$$

because $\bar{I}_\lambda(\underline{x},t)$ is independent of Ω and the integral of the delta function is equal to one. Then, for one-dimensional, one directional models:

$$\bar{I}_\lambda(y,t)=G_\lambda(y,t)\qquad(67)$$

The LVRPA for the photolytic reaction is obtained from:

$$e_\lambda^{a,D}(y,t)=\kappa_{D,\lambda}G_\lambda(y,t)=$$

$$=\kappa_{D,\lambda}(t)\,G_{W,\lambda}\,\exp\left[-\kappa_{T,\lambda}(t)\,y\right]\qquad(68)$$

In Eq. (68) $\kappa_{D,\lambda}$ is the absorption coefficient of 2,4-D exclusively. The boundary condition for Eq. (68) is the Incident Radiation at y = 0. It can be precisely evaluated with actinometer measurements. Potassium ferrioxalate was used according to the operating conditions reported by Murov [Murov *et al.*, 1993]. According to Eq. (9) a mass balance for the well-stirred, isothermal, batch reactor applied to the actinometer reaction gives for the reaction product (Fe^{2+}):

$$\frac{dC_{Fe^{2+}}(t)}{dt}=\left\langle R_{Hom,i}(\underline{x},t)\right\rangle_{V_R}=\Phi_\lambda^{Ac}\left\langle e_\lambda^{a,Ac}(\underline{x},t)\right\rangle_{V_R}\qquad(69)$$

$$\left\langle e_\lambda^{a,Ac}(\underline{x},t)\right\rangle_{V_R}=$$

$$=\frac{1}{V_R/A_R}\int_0^{V_R/A_R}\kappa_{Ac,\lambda}(t)\,G_{W,\lambda}\,\exp\left[-\kappa_{T,\lambda}(t)\,y\right]dy\qquad(70)$$

V_R/A_R is the radiation path. Note that attenuation is influenced by the total absorption coefficient $\left(\kappa_T=\kappa_{Ac}+\kappa_{Fe^{2+}}\right)$ but the reaction rate for the product formation is influenced by the absorption coefficient of the reactant exclusively (κ_{Ac}). Also note that both absorption coefficients are a function of t, because always $\kappa_i=\kappa_i^*C_i$ and C_i for both, Fe^{3+} and Fe^{2+}, changes with the reaction evolution. Integrating Eq. (70) and substituting the results into Eq. (69):

$$\frac{dC_{Fe^{2+}}}{dt}=\Phi_\lambda^{Ac}\,\frac{A_R G_{W,\lambda}}{V_R}\,\frac{\kappa_{Ac,\lambda}(t)}{\kappa_{T,\lambda}(t)}\times$$

$$\left\{1-\exp\left[-\kappa_{T,\lambda}(t)\,(V_R/A_R)\right]\right\}\qquad(71)$$

In Eq. (71) Ac is the reactant (Fe^{+3}) and the reaction product is Fe^{+2}. In the batch reactor, for not too high reactant conversions the plot of Fe^{+2} vs. time gives a straight line. At $t\to 0$, $\left(dC_{Fe^{2+}}/dt\right)_{t\to 0}=m_{Ac}^0$ is the slope of such a straight line. At time $\to 0$, the following equation holds:

$$m_{Ac}^0=\Phi_\lambda^{Ac}\,\frac{A_R G_{W,\lambda}}{V_R}\qquad(72)$$

Eq. (72) is valid because (i) when $t\to 0$, $\kappa_{Fe^{2+},\lambda}=\kappa^*_{Fe^{2+},\lambda}C_{Fe^{2+}}\cong 0$ (the reaction product) and (ii) at λ = 253.7 nm, $\kappa_{T,\lambda}\cong\kappa_{Ac,\lambda}$ for this actinometer is very large. From the experimental results:

$$G_{W,\lambda} = \left(\frac{V_R}{\Phi_\lambda^{Ac} A_R}\right) \lim_{t\to 0}\left(\frac{C_{Fe^{2+}} - C^0_{Fe^{2+}}}{t-0}\right) =$$

$$= \left(\frac{V_R}{\Phi_\lambda^{Ac} A_R}\right) m^0_{Ac} \qquad (73)$$

VI.1.2 *2,4-D Mass Balance*

The reactor operates under the following conditions: (i) perfect mixing and (ii) isothermal performance. The mass balance [Eq. (9)] gives:

$$\frac{dC_D(t)}{dt} = \left\langle R_{D,\lambda}(y,t)\right\rangle_{V_R/A_R}$$

$$C_D(t=0) = C_D^0 \qquad (74)$$

The radiation field is not uniform and consequently the LVRPA is a function of y and so is R_D. Then, in Eq. (74) an average reaction rate has been defined according to:

$$\left\langle R_{D,\lambda}(y,t)\right\rangle_{V_R/A_R} = \frac{A_R}{V_R}\int_0^{V_R/A_R} R_D(y,t)\,dy \qquad (75)$$

An expression for the local reaction rate is still unknown. It was proposed the following general and perhaps too simple relationship:

$$R_{D,\lambda}(y,t) = -\Phi_{D,\lambda}\left[e_\lambda^{a,D}(y,t)\right]^n \left[C_D(t)\right]^m \qquad (76)$$

As it will become clear further ahead, in Eq. (76), within the limits of the performed work, $\Phi_{D,\lambda}$ is an overall quantum yield for the decomposition of 2,4-D. Employing Eq. (68) the average reaction rate results:

$$\left\langle R_{D,\lambda}(y,t)\right\rangle_{V_R/A_R} =$$

$$= -\Phi_{D,\lambda}\frac{A_R}{V_R}\int_0^{V_R/A_R}\left\{\kappa_{D,\lambda}(t) G_{W,\lambda} \times \right.$$

$$\left.\exp\left[-\kappa_{T,\lambda}(t)y\right]\right\}^n \left[C_D(t)\right]^m dy \qquad (77)$$

Substituting into the mass balance:

$$\frac{dC_D(t)}{dt} = -\frac{A_R}{V_R}\Phi_{D,\lambda}\left(G_{W,\lambda}\right)^n \left(\kappa_{D,\lambda}(t)\right)^n \left[C_D(t)\right]^m \times$$

$$\int_0^{V_R/A_R}\left\{\exp\left[-\kappa_{T,\lambda}(t)\,y\right]\right\}^n dy \qquad (78)$$

Since in Eq. (78) the concentration of 2,4-D is uniform it was possible to take it out of the integral. Integrating the right hand side of Eq. (78):

$$\frac{dC_D(t)}{dt} = -\frac{A_R}{V_R}\Phi_{D,\lambda}\left(G_{W,\lambda}\right)^n \frac{\left(\kappa_{D,\lambda}(t)\right)^n}{\kappa_{T,\lambda}(t)n}\left[C_D(t)\right]^m \times$$

$$\left\{1 - \exp\left[-\kappa_{T,\lambda}(t)\,n\left(V_R / A_R\right)\right]\right. \qquad (79)$$

This ordinary differential equation must be solved with the initial condition indicated in Eq. (74). Note that due to the required averaging procedure, the reaction order with respect to the LVRPA (n) has a rather complex relationship with respect to the time rate of change of concentrations. **Since this averaging procedure is required every time that the radiation field is not uniform, in photochemical reactors, graphical methods to obtain this reaction order are useless.** The exception could be the case of very weak radiation absorption.

VI.1.3 *Absorption Coefficients*

Eq. (79) needs two optical parameters that must be obtained from independent measurements. The 2,4-D absorption coefficient can be obtained from standard measurements. The data for 253.7 nm produced a value of the molar *Napierian* absorptivity of 409 L mole^{-1} cm^{-1}. Then, from Beer's equation:

$$\kappa_{D,\lambda} = \overset{*}{\kappa}_{D,\lambda} C_D \qquad (80)$$

To obtain the total absorption coefficient (a mixture of reactant and reaction products) it was proposed:

$$\kappa_{T,\lambda}(t) = \kappa^*_{D,\lambda} C_D(t) + \kappa^*_{Pr,\lambda}\, C_{Pr}(t) \qquad (81)$$

The "unknown-products" hypothetical concentration can be expressed in terms of the 2,4-D instantaneous concentration:

$$\kappa_{T,\lambda}(t) = \kappa^*_{D,\lambda} C_D(t) + \kappa^*_{Pr,\lambda}\left[C^0_D - C_D(t)\right] \qquad (82)$$

$$\kappa_{T,\lambda}(t) = \left[\kappa^*_{D,\lambda} - \kappa^*_{Pr,\lambda}\right] C_D(t) + \kappa^*_{Pr,\lambda} C^0_D \qquad (83)$$

In Eq. (83) only one parameter is unknown. Values of $\kappa_{T,\lambda}$ as a function of $C_D(t)$ were obtained (with spectrophotometric measurements) from all the experimental decomposition runs at 253.7 nm. Applying a linear regression to the experimental points and expressing $\kappa_{T,\lambda}$ in cm^{-1} and $C_D(t)$ in ppm, the following empirical correlation was obtained:

$$\kappa_{T,\lambda}(t) = 0.0197 C^0_D - [0.03755 - 0.0197] C_D(t) \qquad (84)$$

VI.1.4. *Parameter Evaluation*

It is now possible to obtain the kinetic parameters from the experimental data and the proposed kinetic model in Eq. (79). We have three unknowns: the quantum yield, and the exponents "m" and "n". The whole model was fed to a multiparameter, non-linear regression algorithm that is coupled with an optimization program according to the Marquardt method [Marquardt, 1963].

The regression program gave the following values for the exponents: $n \cong 1$ and $m \cong 0$. With these estimations, at 25 C and 253.7 nm, the following kinetic equation was obtained:

$$R_{D,\lambda}(y,t) = -0.0262\, e^{a,D}_{\lambda}(y,t) \qquad (85)$$

Eq. (85) indicates that at 253.7 nm, and for the explored range of concentrations, the overall quantum yield is 2.62%, which is a rather low value. This equation also indicated that the dependence upon the 2,4-D concentration is completely accounted for with the concentration dependence of the LVRPA. However, this result should not be interpreted as zero order dependence with respect to 2,4-D concentration because it participates in two parts of the variable $e^{a,D}_{\lambda}$. From Eqs. (79), (80) and (81) it can be seen that the LVRPA bears a direct linear dependence with the 2,4-D concentration [Eqs. (79) and (80)] and a decreasing exponential dependence with the total absorption coefficient that includes the 2,4-D concentration [Eqs. (79) and (81)]. The inner filtering effect produced by the reaction products is also taken into account by the exponential term.

VI.2. ***Reactor Analysis***

A pilot-plant scale, tubular (annular configuration) photoreactor for the direct photolysis of 2,4-D has been modeled [Martín *et al.*, 1997]. A tubular germicidal lamp was placed at the reactor centerline. This reactor can be used to test, with a very different reactor geometry, the kinetic expression previously developed in the cylindrical, batch laboratory reactor irradiated from its bottom and to validate the annular reactor modeling for the 2,4-D photolysis. Note that the radiation distribution and consequently the field of reaction rates in one and the other system are very different.

It is well known that modeling can be done in two different forms: (i) the **design mode** [to calculate the size (or reaction time) of the reactor for a defined performance] or (ii) **the predictive mode** (to predict the performance of a prescribed reactor). The second approach will be illustrated here. With this approach, the reactor dimensions, the lamp dimensions and its operating characteristics are pre-established conditions. The design mode uses the same methodology but must iterate with different lamp and reactor sizes until the desired performance is satisfied. Iteration is needed because normally, lamp sizes and lamp output powers can not be changed in a continuous manner and the design must

use what is available in the market. Since the reaction is quite slow, the annular reactor will be operated inside a batch recycling system.

VI.2.1. *Proposed reactor (Pilot plant-scale)*

Figures 1 and 3 provide a schematic representation of the employed reacting system. More details can be found in Table N° 1.

VI.2.2. *Reactor Model*

The reactor model was constructed according to the following sequence: (i) The annular reactor, *radiation distribution model* of Romero *et al.* [Romero *et al.*, 1983] was adapted for this particular set-up; (ii) The tubular lamp with voluminal and isotropic *radiation emission model* of Irazoqui *et al.* [Irazoqui *et al.*, 1973] was applied to this system (it is a refinement of the model described in section V); (iii) A *mass balance* for an actinometric reaction carried out in a tubular reactor inside the loop of a recycling system was adapted from Martín *et al.* [Martín *et al.*, 1996], and (iv) To verify the radiation model, actinometer experiments were performed in the reactor to compare theoretical predictions with actual results. This procedure permitted to verify the quality of the radiation emission model for the lamp and the radiation distribution model for the annular reactor. Afterwards, for the photolytic reactor employing 2,4-D the following sequence was followed: (1) A *species mass balance* for a tubular reactor inside the recycling system was written according to Eq. (15); (2) The *kinetic expression* given by Eq. (85) was incorporated into this mass balance; (3) The *radiation model* previously validated was used to predict the LVRPA in the kinetic expression [Eq. (85)]; (4) *Radiation absorption by reaction products* was incorporated into the radiation model according to the empirical expression represented by Eq. (84); (5) Time evolution concentrations of the 2,4-D in the recycling system were predicted using steps (1), (2), (3) and (4); and (6) Experimental 2,4-D concentrations in the pilot plant reactor were compared with theoretical predictions.

Table N° 1

	Parameter	Value	
Reactor	Irradiated length	48	cm
Pyrex®	Outside diameter	6.03	cm
Suprasil®	Inside diameter	4.45	cm
	Irradiated volume	624	cm^3
LAMP	Input power	30	W
Philips TUV	Output power	9	W
λ = 253.7 nm	Nominal length	89.5	cm
	Diameter	2.6	cm
Reservoir	Volume	6000	cm^3

VI.2.3. *Radiation Field*

For a homogeneous medium the radiation distribution is obtained by solving Eq. (34) with the following boundary condition:

$$I_{\lambda,\underline{\Omega}}(s=0) = I^0_{\lambda,\underline{\Omega}} \qquad (86)$$

The boundary condition was obtained from the Extended Source with Voluminal and Isotropic Emission model [Cassano *et al.*, 1995], according to:

$$I^0_\lambda\left[\underline{x}, \underline{\Omega}(\theta,\phi)\right] = \frac{P_\lambda Y_{R,\lambda}(\underline{\Omega})}{2\pi^2 R_L^2 L_L} \frac{\left(R_L^2 - r^2\sin^2\phi\right)^{1/2}}{\sin\theta} \qquad (87)$$

Figure 7 illustrates the principal variables. P_λ is the corresponding output power for the useful lamp length and $Y_{R,\lambda}(\underline{\Omega})$ is the compounded transmission coefficient of the reactor wall (internal absorption plus interfacial reflections). This equation is valid for arc type lamps that have transparent walls, as it is the case of the germicidal lamps employed in this work. It permits the inclusion of all lamp characteristics and the reactor and lamp geometric arrangement into the design of the reactor. The solution of Eq. (34) provides values of the radiation intensity as a function of position (r, z) and direction (θ, ϕ). Once I_λ is known, the Inci-

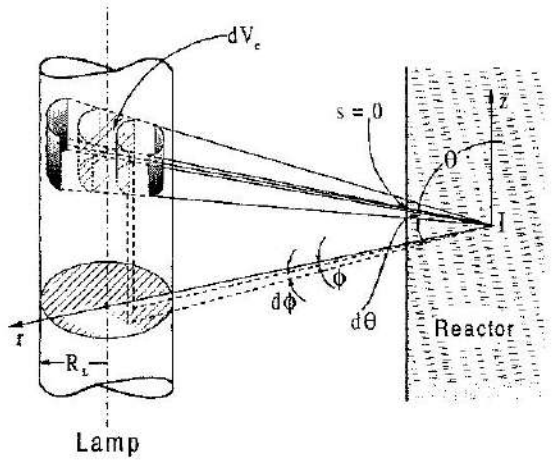

Fig. 7. The Extended Source with Voluminal and Isotropic Emission model. Adapted from (23).

dent Radiation and the LVRPA can be obtained from Eqs. (36) and (38). Since monochromatic radiation is employed, no integration over wavelength is needed. The final equation for calculating the LVRPA is:

$$e^a_\lambda(\underline{x},t)=\frac{\kappa_{i,\lambda}(\underline{x},t)Y_{R,\lambda}(\underline{\Omega})\,P_\lambda}{2\pi^2R_L^2L_L}\times$$

$$\int_{\phi_1}^{\phi_2}d\phi\int_{\phi_1}^{\phi_2}d\theta\left(R_L^2-r^2\sin^2\phi\right)^{1/2}\times$$

$$\exp\left[-\kappa_{T,\lambda}\left(\frac{r\cos\phi-\left(r^2\cos^2\phi-\left(r^2-r_{R,i}^2\right)\right)^{1/2}}{\sin\theta}\right)\right] \tag{88}$$

The integration limits for θ and ϕ for the case of the annular reactor (Fig. 8), were derived by Irazoqui *et al.* [Irazoqui *et al.*, 1973]:

$$\theta_1(\phi)=\tan^{-1}\left\{\frac{r\cos\phi-\left[r^2\left(\cos^2\phi-1\right)+R_L^2\right]^{1/2}}{(L_L-z)}\right\} \tag{89}$$

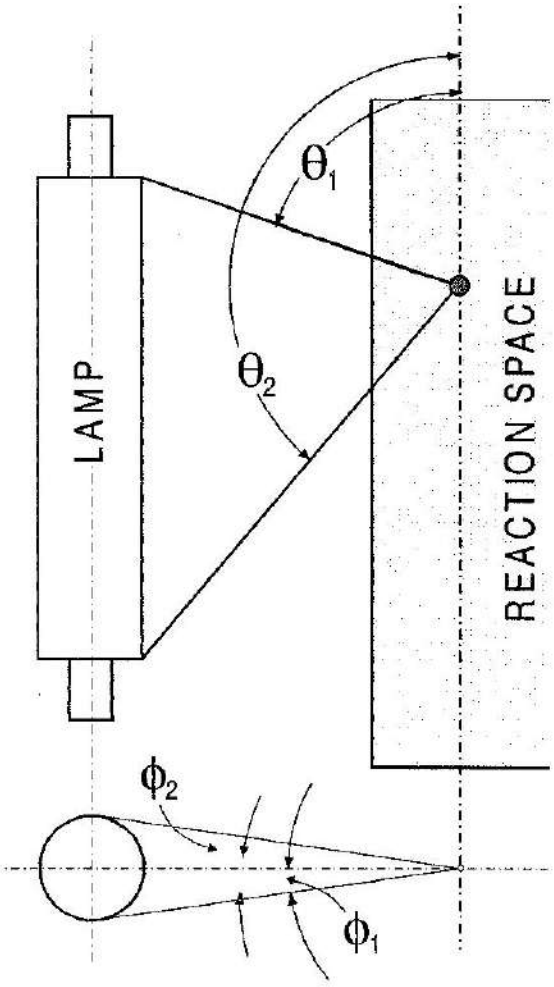

Fig. 8. The integration limits for θ and ϕ angles.

$$\theta_2(\phi)=\tan^{-1}\left\{\frac{r\cos\phi-\left[r^2\left(\cos^2\phi-1\right)+R_L^2\right]^{1/2}}{-z}\right\} \tag{90}$$

$$-\phi_1=\phi_2=\cos^{-1}\left[\frac{\left(r^2-R_L^2\right)^{1/2}}{r}\right] \tag{91}$$

It must be noticed that the exponential term (attenuation) uses the reacting medium *total absorption coefficient* while only the *reactant absorption coefficient* in-

tervenes, with a linear effect, in the value of the LVRPA. Hence "i" stands for the reactant, while:

$$\kappa_{T,\lambda} = \sum_j \kappa_{j,\lambda} \qquad (92)$$

and "j" stands for the reactant and any other component in the reacting medium.

The Actinometer Reaction in the Annular Reactor

The classic uranyl oxalate reaction was used [Murov *et al.*, 1993]. According to Eq. (15), under steady operating conditions, changes in concentration inside the recycling system are obtained from:

$$\left.\frac{dC_i(t)}{dt}\right]_{Tk} = \frac{V_R}{V_{Total}} \left\langle R_{Hom,i}(r,z,t)\right\rangle_{V_R}$$

$$C_i(0) = C_i^0 \qquad (93)$$

This equation is valid when: (1) the recirculation rate is very high and (2) the operation of the reactor is differential. For the actinometer reaction, with i = Ac:

$$R_{Hom,Ac}(r,z,t) = -\Phi_{Ac,\lambda} e_\lambda^{a,Ac}(r,z,t) \qquad (94)$$

Recall that since the radiation field is not uniform in Eqs. (93) and (94) the reaction rate is a function not only of time but of position as well. Then, even for the differential reactor operation a volume average operation is required. For the actinometer reaction this average is easily computed because for conversions below 20%, the reaction rate is not a function of the oxalic acid concentration and the uranyl ion concentration remains constant (a sensitized reaction). Calculating the volume average of the LVRPA we get:

$$\left\langle e_\lambda^{a,Ac}(\underline{x})\right\rangle_{V_R} = \frac{\kappa_{Ac,\lambda}\, Y_{R,\lambda}\, P_\lambda}{\pi R_L^2\, L_L\, V_R} \int_{r_{R,i}}^{r_{R,o}} r dr \times$$

$$\int_0^{L_R} dz \left\{ \int_{\phi_1}^{\phi_2} d\phi \int_{\theta_1}^{\theta_2} d\theta \left(R_L^2 - r^2 \sin^2\phi\right)^{1/2} \times \right.$$

$$\left. \exp\left[-\kappa_{Ac,\lambda} \left(\frac{r\cos\phi - \left(r^2\cos^2\phi - \left(r^2 - r_{R,i}^2\right)\right)^{1/2}}{\sin\theta} \right) \right] \right\} \qquad (95)$$

Molar absorptivities to calculate $\kappa_{Ac,\lambda}$ can be measured in the spectrophotometer and the quantum yield at 253.7 nm can be taken from Murov *et al.* [Murov *et al.*, 1993]. To validate the radiation model, results obtained from of Eq. (95) must be compared with experiments. From Eqs. (93) and (94) and after integration:

$$\left[e_\lambda^{a,Ac}\right]_{Exp.} = \frac{\left[C_{Ac}^0 - C_{Ac}(t)\right]}{(t-0)} \frac{V_{Total}}{V_R} \frac{1}{\Phi_{Ac,\lambda}} \qquad (96)$$

Experiments were carried out at three different uranyl sulfate concentrations: 0.005, 0.001 and 0.0005 M. Oxalic acid concentrations were 5 times larger always. Figure 9 shows the experimental

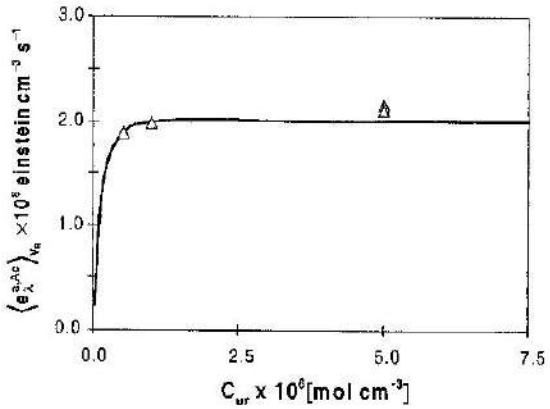

(——) Model predictions [Eq. (95)];

(△) Experimental data [Eq. (96)].

Fig. 9. Experimental verification of the radiation model. Adapted from [Martín et al., 1997].

data [Eq. (96)]. The solid line corresponds to predictions from the radiation and reactor model [Eq. (95)]. The largest error was smaller than 8%. Since agreement is very good, one may conclude that the radiation field of the annular reactor has been precisely represented. Note that no adjustable parameters have been used.

VI.2.4. *The Reactor Model for the 2,4-D Photolysis*

Eq. (93) is the same for the actinometer than for the photolytic reaction, particularly when the reactor differential operation is fulfilled. If the reactor operation is not differential, Eq. (3) with inlet condition (4) and boundary conditions (5) and (6) must be used. Note that the simplified kinetic expression represented by Eq. (85) has the same form as Eq. (94). However, during the 2,4-D photolysis the radiation absorption characteristics of the reacting medium change. This is a very distinct phenomenon because: (i) the uranyl oxalate reaction is a photosensitized reaction and the radiation absorbing species is not consumed and (ii) conversely, not only the 2,4-D absorption coefficient changes but absorption by reaction products increases the total absorption coefficient above the initial value. This phenomenon produces an unavoidable coupling between the steady state radiation balance and the unsteady state mass balance (notice that due to the speed of propagation of the changes in the radiation field, the transient term in the RTE is always negligible). The total absorption coefficient can be obtained from Eq. (84). Then:

$$\frac{dC_D(t)}{dt} = \frac{V_R}{V_{Total}} \left\langle R_{Hom,D}(r,z,t) \right\rangle_{V_R} \qquad (97)$$

with the I.C. $\quad C_D(t=0) = C_D^0$

And the reaction rate is:

$$\left\langle R_{Hom,D}(r,z,t) \right\rangle_{V_R} = -\Phi_{D,\lambda} \frac{1}{V_R} \int_{V_R} e_\lambda^{a,D}(r,z,t)\, dV \qquad (98)$$

Inserting the LVRPA into Eq. (98) and substituting the result into Eq. (97) we obtain:

$$\frac{dC_D}{dt} = -\Phi_{D,\lambda} \frac{1}{V_{Total}} \left[\frac{P_\lambda Y_{R,\lambda} \kappa^*_{D,\lambda} C_D(t)}{\pi R_L^2 L_L} \right] \times$$

$$\int_{r_{R,i}}^{r_{R,o}} r\, dr \int_0^{L_R} dz \left\{ \int_{\phi_1}^{\phi_2} d\phi \int_{\theta_1}^{\theta_2} d\theta \left(R_L^2 - r^2 \sin^2\phi \right)^{1/2} \times \right.$$

$$\left. \exp\left[-\kappa_{T,\lambda} \left(\frac{r\cos\phi - \left(r^2\cos^2\phi - \left(r^2 - r_{R,i}^2 \right) \right)^{1/2}}{\sin\theta} \right) \right] \right\} \qquad (99)$$

$$C_D(t=0) = C_D^0$$

Integration of this equation provides the time evolution of the 2,4-D concentration. Notice that all the lamp characteristics are incorporated in the design. The mass balance and the volume average procedure indicated in the equations above are greatly simplified by the differential operation in the photochemical section of the reactor. Eq. (99) must be numerically solved. At each different time, the LVRPA must be calculated according to the existing concentrations. The most difficult and time-consuming step is the calculation of the Eq. (88) for each reaction condition.

Figure 10 shows the results for two initial concentrations. Solid lines correspond to predictions of the 2,4-D concentrations obtained from the solution of Eq. (99). Symbols correspond to experimental values. It can be seen that agreement is fairly good. The observed discrepancies, that in some cases produce an error as large as 15% are mainly due to the fact that the reaction kinetics of this very complex reaction has been modeled in terms of just one single variable (the 2,4-D concentration). Rigorously speaking, in the case of the 2,4-D reaction one should expect that: (i) more than

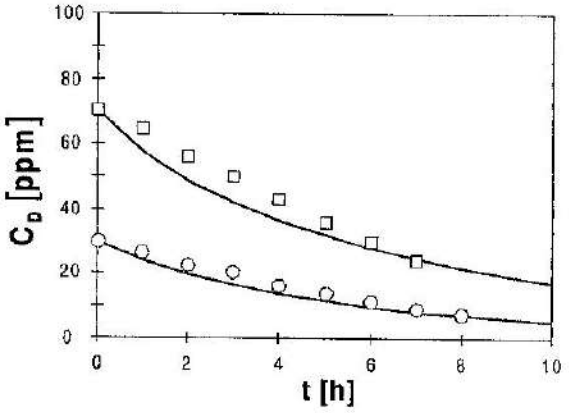

(——) Model predictions;

(□,○) Experimental data.

Fig. 10. 2,4-D concentration vs. time for two initial concentrations. Adapted from [Martín et al., 1997].

one reaction product may affect the radiation absorption of the reacting medium [Eq. (84)] and (ii) the proper reaction kinetics may be a function of other variable besides the LVRPA; for example, intermediate product concentrations [Eq. (85)].

The ideas described in this section can be easily extended to more complex reacting systems either from the chemistry point of view -for example to include the parallel oxidation reaction with hydrogen peroxide or ozone- or to deal with others lamp-reactor configurations. A comprehensive, tutorial review for homogeneous photochemical reactors has been published [Cassano *et al.*, 1995] that provides most of the required methods.

VII. Heterogeneous systems. Application to quantum yield evaluation in slurry reactors

For the case of photocatalytic reactors employing solid semiconductors and trying to reach a compromise between length and clarity in a detailed application, it seems appropriate to concentrate the effort in describing all the reactor analysis concepts that must be developed to measure true quantum yields in heterogeneous slurry photoreactors. This particular problem permits to show in a rather short extension, most of the main features of heterogeneous photocatalytic reactor modeling. Once the distribution of radiation inside reactors of different geometries is known (see for example, [Romero *et al.*, 1997] for annular reactors and [Brandi *et al.*, 1999] for flat plate reactors) basic concepts already available in the chemical reactor engineering literature [Froment and Bischoff, 1990] can be used to model others reaction and reactor types. A complex reaction scheme or mechanism can also be incorporated into the *corresponding* mass balance as it has been shown by Alfano *et al.* [Alfano *et al.*, 1997] and Cabrera *et al.* [Cabrera *et al.*, 1997 (b)]. A typical example of modeling a different reactor type has been recently published, dealing with a fluidized bed, photocatalytic reactor [Chiovetta *et al.*, 2001].

The general methodology for modeling slurry photoreactors has been reviewed by Cassano and Alfano [Cassano and Alfano, 2000]. We will apply these concepts to the evaluation of absolute and true values of quantum yields.

VII.1. *Definition of the problem*

The monochromatic, overall, true initial quantum yield is defined as:

$$\left[\Phi_\lambda^0\right]_{TRUE} = \frac{\left\{\left[\text{Rate of}\left\{\begin{matrix}\text{disapearance}\\ \text{appearance}\end{matrix}\right\}\text{of compound "i"}\left(\underline{x},t\right)\right]_\lambda^{t\to 0}\right\}_{V_R-AVER}}{\left\{\left[\text{Rate of photon absorption by the catalyst}\left(\underline{x},t\right)\right]_\lambda\right\}_{V_R-AVER}} = \frac{\left[\left\langle R_i\right\rangle_{V_R}^0\right]_{EXPER}}{\left[\left\langle e_\lambda^a\right\rangle_{V_R}\right]_{CALC}} \qquad (100)$$

The volume average of LVRPA is very difficult to measure. However, employing rigorous mathematical modeling of

photocatalytic slurry reactors it can be precisely calculated [Brandi *et al.*, 2000 (a); Brandi *et al.*, 2000 (b)]. Consequently, in Eq. (100): (i) the numerator is the reactor volume-average of the reaction rate measured at initial conditions (the result of an experimental determination), (ii) the denominator is the reactor volume-average of the **calculated** spatial distribution of the LVRPA, and (iii) the LVRPA is calculated solving the Radiative Transfer Equation (RTE) employing catalyst optical properties and light intensities arriving at the reactor window for radiation entrance, both independently measured.

Quantum yields are not unique values unless several operating conditions are precisely defined, for example:

1. Concerning the employed radiation: (1.1) wavelength must be monochromatic and (1.2) the employed range of radiation intensities must be defined because of the existence of different reaction order dependencies at different irradiation rates.

2. Concerning the reaction environment, several conditions must be fixed: (2.1) temperature, (2.2) pH, (2.3) substrate initial concentration, and (2.4) quality of the "reactants" that are employed because impurities affect the photocatalytic rates.

3. Concerning the oxidative path: operating conditions must ensure excess oxygen concentration over the stoichiometric demand during the full course of the reaction.

4. Concerning the catalyst we must define: (4.1) catalyst variety and (4.2) catalyst concentration.

Additionally, to facilitate comparisons, quantum yields should be measured at substrate and catalyst concentrations where the reaction rate shows zero order dependence with respect to both variables.

VII.2. *Methodology*

To develop a rigorous model of a photocatalytic slurry reactor several steps were necessary. They are briefly described below.

1. To study scattering effects by solid particles in a fluid and adapt previous existing methods in generalized transport theory (the Discrete Ordinate Method or DOM) [Duderstadt and Martin, 1979] to solve the RTE [Alfano *et al.*, 1995].

2. To develop a laboratory reactor that permits the easiest solution of the RTE employing the DOM [Cabrera *et al.*, 1994]. It consists of a flat plate configuration (a cylinder irradiated from one of its circular surfaces).

3. To develop special methods to measure monochromatic specific (per unit catalyst mass) absorption (κ_λ^*) and scattering (σ_λ^*) coefficients of titanium dioxide slurries and obtain values for different catalysts and for the wavelength range between 295 and 395 nm [Cabrera *et al.*, 1996].

4. To develop precise methods for obtaining intrinsic kinetic data in a batch reactor with recycle [Alfano *et al.*, 1997; Cabrera *et al.*, 1997 (b)]. It includes a model for radiation absorption by a *material particle* (in the continuous mechanics definition) made of catalytic particles and the fluid. The model has the ability of separating and calculating radiation absorption by any of the two phases. Thus, parallel photolysis can be also handled.

5. To include effects of reactor wall properties into the incident radiation intensities corresponding to the boundary condition for radiation entrance. The model includes internal absorption and interfacial reflectivities [Brandi *et al.*, 1999].

6. To characterize and model the problem of reactor window fouling by titanium dioxide [Brandi *et al.*, 1999].

7. To select the best phase function for radiation scattering by titanium dioxide [Brandi *et al.*, 1999].

8. To obtain direct and precise experimental verification of the quality of the results obtained with the numerical solution of the RTE with the DOM [Brandi *et al.*, 2000 (a); Brandi *et al.*, 2000 (b)]. For catalyst loadings above 0.25 g/L, errors were never larger than 5%.

VII.3. ***Selection of a reactor***

At this point we should decide on the experimental reactor to be used. Cabrera *et al.* [Cabrera *et al.*, 1994] proposed a new experimental reactor that --with a few changes– has been also successfully used for detailed kinetic studies. Figure 11 gives a schematic description of the device. It is made of the following parts:

1. A cylindrical reactor with two flat windows made of good quality Pyrex glass (alternatively, one of them may be made of Suprasil quality quartz). The window for radiation entrance –either glass or quartz– must be modified; its external side upon abrasion with HF has the texture of ground glass. The reactor has an optical path (L_R) sufficiently large to ensure that no radiation is arriving at the flat plate facing the window of radiation entrance. With a length of 10 cm, the reactor volume is 212 cm^3. Illuminating the reactor through the modified window produces diffuse irradiation inside (the irradiation boundary condition) which greatly simplifies the radiation model (Fig. 11).

2. A tubular UV lamp of well-known characteristics: output power, radiation spectral distribution of its output energy and geometrical dimensions. It is a 360 W, UA3-UVIARC lamp, from G.E. Its operation can be continuously monitored with a W-A-V meter. This lamp has significant peaks of emission at 313 and 365 nm.

3. A cylindrical reflector of parabolic cross-section with well-known reflecting properties (Alzak® from Alcoa) and well-defined geometrical dimensions. The lamp is placed at its focal axis and the distance from the reflector to the reactor is precisely measured and controlled.

4. Monochromatic light was obtained by interposing in the radiation bundles trajectories narrow band interference filters (peaks at 313 nm and 365 nm). To protect the filters, an infrared absorbing filter was placed between the lamp and the interference filter holder.

5. A shutter placed in front of the reactor window permitted to decide on the exact starting time of the reaction once steady state conditions had been reached.

6. A calibrated photodiode detector with a filter connected by means of a quartz optical fiber to an UV radiometer was placed by the reactor window opposite to the one of radiation entrance. It permitted monitoring of the lamp operation and the conditions of both reactor windows as a consequence of the unavoidable fouling produced by Degussa P 25 titanium dioxide.

The reacting system was operated inside the loop of a batch recycling arrangement (Fig. 12) with provisions for: (1) a storage tank made of glass with a volume of 2100 cm^3, (2) an all glass and Teflon recirculating pump with high flowrate capacity, (3) a device for the exact positioning of the reactor and the reflector (with the lamp), (4) a temperature control system, (5)

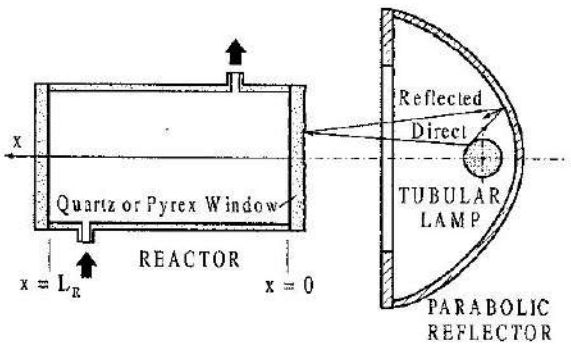

Fig. 11. Schematic description of the unidimensional photocatalytic reactor. Adapted from [Alfano et al., 1997].

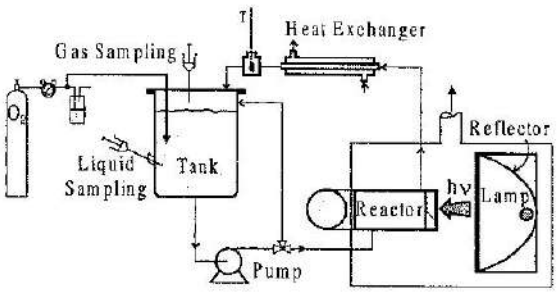

Fig. 12. Flow sheet of the experimental device. Adapted from [Cassano and Alfano, 2000].

a continuous feed for oxygen, (6) two sampling ports in the tank: for the headspace and for the liquid, (7) a stirring system for the tank, and (8) an exhausting system.

A laboratory reactor must be constructed in such a way that an exact analysis of the experimental results should be simplified as much as possible. This experimental device has four important features for its modeling: (1) the tank volume is significantly larger than the reactor volume, (2) the pump has a high flowrate; thus in the reactor, conversion per pass will be very small, (3) irradiation at the inside face of the reactor window is diffuse which means that azimuthal symmetry for the direction of radiation propagation inside the reactor will be achieved, and (4) no radiation arrives at the opposite face of the reactor plate and consequently there is no radiation reflection on this face. The first two characteristics simplify the mass balance and the other two have the same effect on the radiation balance.

VII.4. *Calculating procedure for the reaction rate*

Consider the case represented in Figure 12. From Eq. (1), a local mass balance for the i-component **in the liquid where there is no chemical reaction** (no parallel photolysis) is:

$$\frac{\partial C_i(\underline{x},t)}{\partial t} + \underline{\nabla}\cdot\underline{N}_i = 0 \qquad (101)$$

This equation can be integrated over the whole **liquid** volume of the system ($V_{L,T}$) that, in principle, is different from the total volume of the suspension (liquid + solid) ($V_{Tot} = V_{Tk} + V_R = V_{L,T} + V_{S,T}$):

$$\int_{V_{L,T}} \frac{\partial C_i(\underline{x},t)}{\partial t}\,dV + \int_{V_{L,T}} \underline{\nabla}\cdot\underline{N}_i\,dV = 0 \qquad (102)$$

Note that V_{Tk} includes all volumes in the system that are not the photocatalytic reactor volume. Since the total volume is fixed (integration limits are not a function of time):

$$\int_{V_{L,T}} \frac{\partial C_i(\underline{x},t)}{\partial t}\,dV = \frac{d}{dt}\int_{V_{L,T}} C_i(\underline{x},t)\,dV \qquad (103)$$

The second integral can be divided in two parts: (i) one comprising the liquid volume of the reactor and (ii) the other comprising the liquid volume of the tank. In the first part we can apply the definition of an average concentration and in the second we must recognize that the concentration of the tank is uniform. Since:

$$\langle C_i(\underline{x},t)\rangle_{V_{L,R}} = \frac{1}{V_{L,R}}\int_{V_{L,R}} C_i(\underline{x},t)\,dV \qquad (104)$$

$$\int_{V_{L,T}} \frac{\partial C_i(\underline{x},t)}{\partial t}\,dV = V_{L,R}\frac{d}{dt}\langle C_i(\underline{x},t)\rangle_{V_{L,R}} + V_{L,Tk}\left.\frac{dC_i(t)}{dt}\right|_{Tk} \qquad (105)$$

In Eq. (105), $\langle C_i(\underline{x},t)\rangle_{V_{L,R}}$ is the reactor liquid volume averaged concentration of component i. In V_{Tk} - a well stirred system - since there is no chemical reaction, $C_i(\underline{x},t)$ is uniform and was directly taken out of the volume integral.

On its turn, the second volume integral of Eq. (102) can be transformed into a surface integral (with the Divergence theorem). Then, applying the definition of the molar flux [Bird *et al.*, 2002 p. 537] it can be written as:

$$\int_{V_{L,T}} \underline{\nabla}\cdot\underline{N}_i\,dV = \int_{A_{S,T}} \left[\underbrace{\underline{J}_i(\underline{x},t)}_{\text{Diffusion}} + \underbrace{C_i(\underline{x},t)\underline{v}}_{\text{Convection}}\right]\cdot\underline{n}_L\,dA \qquad (106)$$

We have considered that $A_{L,T} = A_{S,T}$; i.e., the total interfacial area of the liquid is equal to the total interfacial area of the solid. Noting that fluxes are different from zero only at permeable solid surfaces, in a closed system the only permeable surfaces are those corresponding to the catalyst. In Eq. (106) $\underline{v}$ is the mass averaged liquid velocity. Substituting Eqs. (105) and (106) into Eq. (102):

$$V_{L,R}\frac{d}{dt}\left\langle C_i(\underline{x},t)\right\rangle_{V_{L,R}} + V_{L,Tk}\frac{dC_i(t)}{dt} =$$

$$= -A_{S,T}\left\langle\left[\underline{J}_i(\underline{x},t)\right]\cdot\underline{n}_L\right\rangle_{A_{S,T}} -$$

$$-\int_{A_{S,T}} C_i(\underline{x},t)\,\underline{v}\cdot\underline{n}_L\,dA \qquad (107)$$

In Eq. (107) $\left\langle\left[\underline{J}_i(\underline{x},t)\right]\cdot\underline{n}_L\right\rangle_{A_{S,T}}$ is ***"the total liquid-solid particles interface, averaged, molar diffusive flux of component i"***. Note that $A_{S,T} = A_{S,R} + A_{S,Tk}$. The second term of the right hand side of Eq. (107) is zero because at the catalyst interface convective fluxes are zero. On the other hand, from Eq. (18) the molar diffusive flux through the boundary layer at the liquid-solid interface must be equal to the reaction rate at the liquid-solid interface:

$$A_{S,T}\left\langle\underline{J}_i(\underline{x},t)\cdot\underline{n}_L\right\rangle_{A_{S,T}} = A_{S,R}\left\langle\underline{J}_i(\underline{x},t)\cdot\underline{n}_L\right\rangle_{A_{S,R}} =$$

$$= -A_{S,R}\left\langle R_{Het,i}(\underline{x},t)\right\rangle_{A_{S,R}} \qquad (108)$$

In Eq. (108) the molar flux at the solid-liquid interface is different from zero only at the permeable solid-liquid interface where there is chemical reaction; this means that this flux is different from zero only at $A_{S,R}$. Substituting Eq. (108) into Eq. (107):

$$\varepsilon_L\frac{V_R}{V_{Tk}}\frac{d\left\langle C_i(\underline{x},t)\right\rangle_{V_{L,R}}}{dt} + \varepsilon_L\frac{dC_i(t)}{dt} =$$

$$= \frac{V_R}{V_{Tk}}a_V\left\langle R_{Het,i}(\underline{x},t)\right\rangle_{A_{S,R}} \qquad (109)$$

In Eq. (109) the following definitions have been used:

$$\frac{V_{L,R}}{V_R} = \frac{V_{L,Tk}}{V_{Tk}} = \varepsilon_L \qquad (110)$$

$$A_{S,R} = a_V\,V_R \qquad (111)$$

where ε_L is the liquid hold-up in the system that is uniform throughout, and a_V is the catalytic surface area per unit suspension volume. Since $V_R/V_{Tk} < 1$ and the conversion per path in the reactor $\left[\frac{d\left\langle C_i(\underline{x},t)\right\rangle_{V_{L,R}}}{dt}\right]$ is very small (both being design conditions):

$$\varepsilon_L\left.\frac{dC_i(t)}{dt}\right|_{Tk} = \frac{V_R}{V_{Tk}}a_V\left\langle R_{Het,i}(\underline{x},t)\right\rangle_{A_{S,R}} \qquad (112)$$

Since:

$$a_V = S_g\,C_{mp} \qquad (113)$$

the reaction rate per unit catalytic surface area results:

$$\left\langle R_{Het,i}(\underline{x},t)\right\rangle_{A_{S,R}} =$$

$$= \varepsilon_L\frac{1}{S_g\,C_{mp}}\frac{V_{Tk}}{V_R}\left.\frac{dC_i(t)}{dt}\right|_{Tk}\;[=]\;\frac{mol}{cm^2\,s} \qquad (114)$$

When the same value per unit suspension volume is needed [for Eq. (100)] we must consider that (i) the cross sectional area corresponding to the irradiated flat plate reactor is constant (a design condition) and (ii) the catalyst concentration is uniform (well mixed system in the whole reactor volume; a established operating condition):

$$\left\langle R_{Het,i}(\underline{x}.t)\right\rangle_{V_R}^{Pseudo} = \left\langle R_{Het,i}(\underline{x}.t)\right\rangle_{L_R}^{Pseudo} =$$

$$= \varepsilon_L\frac{V_{Tk}}{V_R}\left.\frac{dC_i(t)}{dt}\right|_{Tk}\;[=]\;\frac{mol}{cm^3\,s} \qquad (115)$$

In Eqs. (114) or (115) we need to measure dC_i/dt in the tank because all other values are known. Note that the above described conditions permitted to move from the average reaction rate over the surface area of

the solid catalyst to the average over the reactor volume; and for the one-dimensional model, to the average over the reactor length.

$$\langle R_{Het,i}\rangle_{AS,R}\ a_V = \langle R_{Het,i}\rangle_{V_R}^{Pseudo} = \langle R_{Het,i}\rangle_{LR}^{Pseudo} \tag{116}$$

Eq. (115) can be integrated with the initial condition:

$$t = 0 \quad \rightarrow C_i = C_i^0 \tag{117}$$

Eq. (115) provides the value of the numerator for Eq. (100). For calculating initial rates, the time rate of change of the substrate concentration must be calculated as $t \rightarrow 0$. It will be seen that this evaluation is greatly simplified for the conditions that will be defined for calculating quantum yields (Section VII.6).

VII.5. *Photon absorption rate by a material particle of the suspension*

At this point we would like to know the LVRPA by the solid and to be able to isolate this value even if the liquid would also absorb radiation. **To do this we need to model absorption by a material particle of the suspension.** In the continuum mechanics sense, a material point in space is a volume for which every property can be well defined by a single value (for example, temperature, density, concentration, etc.). Its size may be very large if the system is uniform and at equilibrium or very small if significant gradients are present. **For a catalytic suspension, it will be made of the liquid and the solid phases.** Let us consider a small volume V of the suspension space representing this material particle. This volume is located at a point in space $\underline{x}$ (Fig. 13). Any point inside V can be defined in terms of a local reference frame $\underline{\varsigma}$. The particles of many of the known varieties of titanium dioxide have a non-porous structure; then, absorption of radiation is produced in the particle volume through its bounding surface that is characterized by a

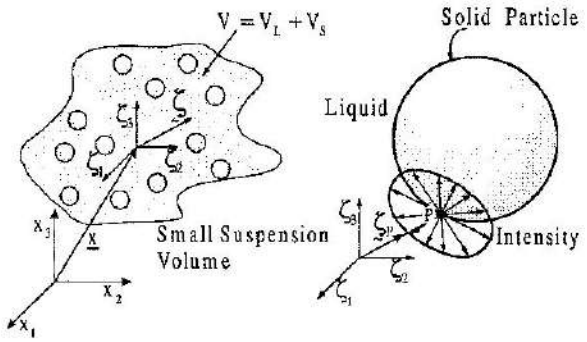

Fig. 13. Modeling of photon absorption by a material particle of the suspension. Adapted from [Cassano and Alfano, 2000].

unit normal vector $\underline{n}_S$, pointing outwards. The Net Radiation Flux is defined as follows:

$$\underline{q}_\lambda(\underline{x}, t) = \int_\Omega I_{\lambda,\Omega}(\underline{x}, t)\underline{\Omega}\, d\Omega \tag{118}$$

Note that the Net Radiation Flux is different for the Incident Radiation because here integration over the solid angle is made with a **vectorial** quantity. The normal component of the Radiation Flux is equal to the Incident Radiation only for one-directional radiation transport. At a given point on the surface of a catalytic particle radiation arrives from different directions in the surrounding space. This energy defines the Radiation Flux vector at point P inside this small volume that is given by:

$$\underline{q}_\lambda\left(\underline{x}+\underline{\varsigma}_P, t\right) = \int_{\Omega=4\pi} I_{\lambda,\Omega}\left(\underline{x}+\underline{\varsigma}_P, t\right)\underline{\Omega}\, d\Omega \tag{119}$$

Part of this radiation may be reflected on the surface (scattered) and part may be absorbed. The flux that is going inside the particle and is absorbed at point $P(\underline{x} + \underline{\varsigma}_P)$ on the differential surface dA of particle "n", at a time t and for a wavelength λ (actually between λ and $\lambda + d\lambda$) is:

$$de^a_{\lambda,Sn}\left(\underline{x}+\underline{\varsigma}_P, t\right) = \left[\underline{q}_\lambda\left(\underline{x}+\underline{\varsigma}_P, t\right)\cdot \underline{n}_L\right] dA =$$

$$= \left[\int_{\Omega=4\pi} I_{\lambda,\Omega}\left(\underline{x}+\underline{\varsigma}_P, t\right)\underline{\Omega}\cdot \underline{n}_L\, d\Omega\right] dA \tag{120}$$

for all positive values of the dot product (fluxes that are not reflected).

If polychromatic radiation is used, Eq. (120) must be integrated over the wavelength interval of the useful radiation range of interest (λ_1 and λ_2), accounting for the overlapping wavelength regions of lamp emission, reactor wall transmission (absorption and reflection) and radiation absorbing catalytic species absorption coefficient. Considering the total external area of the solid particle A_{Sn}:

$$e^a_{\lambda,Sn}(\underline{x},t) = \int_{A_{Sn}} dA\left[\int_{\Omega=4\pi} I_{\lambda,\Omega}\left(\underline{x}+\underline{\zeta}_P,t\right)\underline{\Omega}\cdot\underline{n}_L\right] =$$

$$= \int_{A_{Sn}} dA\left[\underline{q}_\lambda\left(\underline{x}+\underline{\zeta}_P,t\right)\cdot\underline{n}_L\right] \qquad (121)$$

According to Figure 13, $\underline{n}_L$ (the outwardly directed normal to the liquid phase) $= -\underline{n}_S$ (the outwardly directed normal to the solid). Applying the Divergence theorem to Eq. (121) and thus transforming the surface integral into a volume one, we get:

$$e^a_{\lambda,Sn}(\underline{x},t) = \int_{A_{Sn}} dA\left[\underline{q}_\lambda\left(\underline{x}+\underline{\zeta}_P,t\right)\cdot\underline{n}_S\right] =$$

$$= -\int_{V_{Sn}} dV\left[\underline{\nabla}\cdot\underline{q}_\lambda\left(\underline{x}+\underline{\zeta}_P,t\right)\right] \qquad (122)$$

Following Ozisik [Ozisik, 1973, p. 251] we recall Eq. (46):

$$\frac{dI_\lambda}{ds} = \underline{\Omega}\cdot\underline{\nabla}I_{\lambda,\Omega} = \underline{\nabla}\cdot\left(\underline{\Omega}I_{\lambda,\Omega}\right) \qquad (123)$$

Additionally, neglecting emission, we can multiply Eq. (47) by $d\Omega$ and integrate over the whole spherical space ($\Omega = 4\pi$). In- and out-scattering cancel out because:

$$\frac{1}{4\pi}\int_{\Omega=4\pi} p(\underline{\Omega}'\rightarrow\underline{\Omega})d\Omega = 1 \text{ and } \int_{\Omega=4\pi} d\Omega = 4\pi \qquad (124)$$

Considering Eq. (118) and since the $\underline{\nabla}$ is independent of the solid angle, we have:

$$\int_{\Omega=4\pi}\underline{\nabla}\cdot\left(\underline{\Omega}I_{\lambda,\Omega}\right)d\Omega = \underline{\nabla}\cdot\underbrace{\int_{\Omega=4\pi} I_{\lambda,\Omega}\underline{\Omega}\,d\Omega}_{\text{Radiation flux}} = \underline{\nabla}\cdot\underline{q}_\lambda =$$

$$= \underbrace{-\kappa_\lambda\int_{\Omega=4\pi} I_{\lambda,\Omega}\,d\Omega}_{\text{Radiation Absorption}} \qquad (125)$$

The last term in Eq. (125) can be substituted according to:

$$\underline{\nabla}\cdot\underline{q}_\lambda(\underline{x},t) = -e^a_\lambda(\underline{x},t) \qquad (126)$$

where e^a_λ is the Local Volumetric Rate of Photon Absorption (the LVRPA). Had we included emission, the left-hand side of Eq. (126) would have represented the **net** absorption or **net** emission depending on whether it is negative or positive. In this case, we have considered only absorption by the reacting media. Applying Eq. (126) to the case described by Eq. (122), the monochromatic photon absorption rate for particle "n" results:

$$e^a_{\lambda,Sn}(\underline{x},t) = \int_{V_{Sn}} dV e^a_{\lambda,S}\left(\underline{x}+\underline{\zeta},t\right) \qquad (127)$$

In Eq. (127) V_{Sn} is the volume of the "n" solid particle. We must now relate the LVRPA per particle, $e^a_{\lambda,Sn}(\underline{x}+\underline{\zeta},t)$, to the LVRPA by the suspension volume (liquid + solid), $e^a_\lambda(\underline{x},t)$. The absorbed energy per unit wavelength interval, unit time and unit volume of the suspension (solid plus liquid) is by definition of an average value over the total volume:

$$e^a_\lambda(\underline{x},t) = \frac{1}{V}\int_V dV e^a_\lambda\left(\underline{x}+\underline{\zeta},t\right) \qquad (128)$$

V is the small suspension volume of the heterogeneous system (solid plus liquid) located at point $\underline{x}$. The right hand side of Eq. (128) can be divided in two parts: (i) the radiation energy absorbed by the liquid and (ii) that part of the absorbed radiation corresponding to the solid particles:

$$e^a_\lambda(\underline{x},t)=\frac{1}{V}\underbrace{\int_{V_L} dV e^a_{\lambda,L}\left(\underline{x}+\underline{\varsigma},t\right)}_{\text{Absorption by the liquid}}+$$

$$+\frac{1}{V}\underbrace{\int_{V_S} dV e^a_{\lambda,S}\left(\underline{x}+\underline{\varsigma},t\right)}_{\text{Absorption by the solid}} \qquad (129)$$

Suppose that in the small volume V we have "*N*" solid photocatalytic particles; then, the right hand side of Eq. (129) can be changed according to:

$$e^a_\lambda(\underline{x},t)=\frac{1}{V}\int_{V_L} dV e^a_{\lambda,L}\left(\underline{x}+\underline{\varsigma},t\right)+$$

$$+\frac{1}{V}\left[\underbrace{\sum_{n=1}^{N}\int_{V_{Sn}} dV e^a_{\lambda,S}\left(\underline{x}+\underline{\varsigma},t\right)}_{\text{Absorption by one particle}}\right] \qquad (130)$$

Assuming that all particles are equal:

$$e^a_\lambda(\underline{x},t)=\frac{1}{V}\int_{V_L} dV e^a_{\lambda,L}\left(\underline{x}+\underline{\varsigma},t\right)+$$

$$+\frac{N}{V}\int_{V_{Sn}} dV\, e^a_{\lambda,S}\left(\underline{x}+\underline{\varsigma},t\right)=$$

$$=\varepsilon_L\underbrace{\left\langle e^a_{\lambda,L}\left(\underline{x}+\underline{\varsigma},t\right)\right\rangle_{V_L}}_{\substack{\text{Average value of absorption}\\ \text{by the liquid phase}}}+$$

$$+\underbrace{N_V}_{\substack{\text{Number of particles}\\ \text{per unit volume}}}\underbrace{\int_{V_{Sn}} dV e^a_{\lambda,S}\left(\underline{x}+\underline{\varsigma},t\right)}_{\text{Absorption by one particle}} \qquad (131)$$

In this equation ε_L is the liquid hold-up (V_L/V) and $N_V = N/V$ is the number of particles per unit suspension volume. Finally from Eqs. (127) and (131) we get:

$$\underbrace{e^a_{\lambda,Sn}(\underline{x},t)\,N_V}_{\text{Absorption by the solid}}=$$

$$=\left[\underbrace{e^a_\lambda(\underline{x},t)}_{\text{Total absorption}}-\underbrace{\varepsilon_L\left\langle e^a_{\lambda,L}\left(\underline{x}+\underline{\varsigma},t\right)\right\rangle_{V_L}}_{\text{Absorption by the liquid}}\right] \qquad (132)$$

If the liquid does not absorb radiation in the wavelength range under consideration, the second term of the right hand side is zero. Note that:

$$N_V\left(e^a_{\lambda,Sn}\right)=\text{Absorption by all solids in the material volume V} \qquad (133)$$

However, if the liquid absorbs radiation, the complete Eq. (131) will be necessary to compute the radiation field inside the reactor. When this is the case, that part of the radiation absorbed by the liquid must be also incorporated into a **separate initiation rate for the reaction mechanism in the homogeneous phase**. Hence, when absorption by the liquid phase is present, both absorbents produce attenuation of radiation inside the reactor: the liquid and the solid. Then, to model the radiation field in the reactor, radiation attenuation produced by absorption (in both phases, with two separate absorption coefficients) and scattering (in and out) inside the system, must be fully incorporated using an equation that accounts for the addition of the four concomitant processes. Thus, attenuation is affected by the four phenomena (including in and out scattering as part of them) but each one of the different terms for absorption (by the fluid and by the solid) defines a different activation step. Activation of the solid is the only one that is needed to formulate the photocatalytic initiation step. When the liquid is transparent, Eq. (132) indicates that the solution provided by the RTE in terms of the absorption and scattering coefficients of the suspension, can provide, directly, the value of the photon absorption rate by solid particles. Consequently, if the liquid is transparent:

$$\underbrace{e^a_{\lambda,Sol}(\underline{x},t)}_{\substack{\text{Absorption by}\\ \text{the solid particles}}}=N_V e^a_{\lambda,Sn}(\underline{x},t)=$$

$$=\underbrace{e^a_\lambda(\underline{x},t)}_{\text{Solution of the RTE}}\left[\frac{\text{einstein}}{\text{cm}^3\,\text{s}}\right] \qquad (134)$$

VII.6. *Calculating procedure for the LVRPA*

In order to apply Eq. (134) we need to solve the RTE [Eq. (47)] for this particular reactor set up. As shown by Alfano *et al.* [Alfano *et al.*, 1995] and Cabrera *et al.* [Cabrera *et al.*, 1994] the radiation field of this reactor can be modeled with a one-dimensional — one-directional radiation model and rather simple boundary conditions (Fig. 14). Hence, with azimuthal symmetry derived from the diffuse emission at x = 0, since:

$$\frac{d}{ds} = \frac{\partial}{\partial x}\frac{dx}{ds} = \mu\frac{\partial}{\partial x} \quad \text{with } \mu = \cos\theta \qquad (135)$$

We obtain:

$$\mu\frac{\partial I_\lambda(x,\mu)}{\partial x} + (\kappa_\lambda + \sigma_\lambda)I_\lambda(x,\mu) =$$

$$= \frac{\sigma_\lambda}{2}\int_{\mu=-1}^{\mu=1} I_\lambda(x,\mu')\,p(\mu,\mu')\,d\mu' \qquad (136)$$

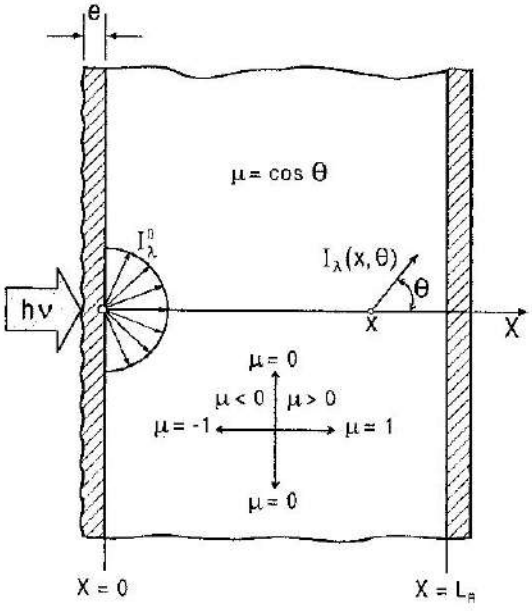

Fig. 14. Radiation field modeling of the one-dimensional, one-directional photoreactor. Adapted from [Cabrera et al., 1996; Cassano and Alfano, 2000].

And the following boundary conditions:

$$I_\lambda(0,\mu) = I^0_\lambda \qquad \mu > 0 \qquad (137)$$

$$I_\lambda(L_R,\mu) = 0 \qquad \mu < 0 \qquad (138)$$

Just one spatial coordinate (x) and one angle (θ) are needed to describe radiation transport in this reactor. Diffuse radiation permit to consider incoming intensities independent of direction [Eq. (137)]. Eq. (138) profits by the fact that no radiation is arriving at $x = L_R$ that translated into zero reflection at that face of the reactor. At this point we need the value of I^0_λ. It can be obtained by two different approaches:

1. With an emission model for the tubular lamp and the parabolic reflector [Alfano *et al.*, 1985; Alfano *et al.*, 1986 (a) and 1986 (b)]. This model, with no adjustable parameters, permits to calculate radiation intensities at any point on the reactor window if the lamp and reflector characteristics and geometric dimensions are known. It takes into account both direct and reflected radiation. These intensities can then be transformed into fluxes [Eq. (118)] and both contributions added at x = 0 - e (with e being the wall thickness). It was found that, with the adopted arrangement, radiation fluxes were fairly uniform on the surface of radiation entrance. They were, however, averaged over the surface of the window, affected by the experimentally measured wall transmission coefficient and transformed into direction independent intensities according to:

$$\langle q_{T,\lambda}(r,\beta)\rangle_{A_R} =$$

$$= \frac{4}{\pi r_R^2}\int_0^{r_R} r\,dr \int_0^{\pi/2} d\beta \left[\underbrace{q_{D,\lambda}(r,\beta)}_{\text{Direct radiation Fluxes}} + \underbrace{q_{RE,\lambda}(r,\beta)}_{\text{Reflected Radiation Fluxes}}\right] \qquad (139)$$

Since radiation is diffuse, intensities can be calculated from:

$$I_\lambda^0 = \frac{1}{\pi} Y_{R,\lambda} \left\langle q_{T,\lambda}(r,\beta) \right\rangle_{\Delta_R} \qquad (140)$$

$Y_{R,\lambda}$ is the compounded transmission coefficient of the reactor window, a function of direction, wavelength, the internal transmittance of the quartz (or glass) and the intervening interfacial reflectivities (air-quartz and quartz-water) or alternatively, it can also be obtained experimentally.

2. The boundary condition may also be directly measured with homogeneous actinometry inside the reactor as it was shown in the previous section of this chapter. It is always possible to use the first method and verify the results with the second, employing the well-known uranyl oxalate or potassium ferrioxalate actinometers.

Eq. (136) with B.Cs. (137) and (138) can be solved with the Discrete Ordinate Method [Duderstadt, 1979]. At this point, absorption and scattering coefficients, as well as the phase function for scattering must be known. They are available from: (i) specific (per unit catalyst mass) absorption and scattering coefficients for different varieties of titanium dioxide in water suspension have been measured by Cabrera *et al.* [Cabrera *et al.*, 1996] as a function of wavelength (Fig. 15); both bearing a linear relationship with the catalyst concentration and (ii) Brandi *et al* [Brandi *et al.*, 1999] have shown that scattering by Degussa P 25 titanium dioxide can be well represented by the isotropic phase function [$p(\mu' \rightarrow \mu) = 1$].

Solution in terms of intensities can be immediately used to calculate local values of the LVRPA. Optical properties can be assumed constant (stable catalyst) and consequently, for a transparent organic compound the κ_λ and σ_λ values are only a function of position at the most. The numerical result gives monochromatic intensities as a function of position and direction. Then the following operations can be performed:

$$G_\lambda(x) = 2\pi \int_{\mu=-1}^{\mu=1} I_\lambda(x,\mu) d\mu \quad [=] \quad \frac{\text{einstein}}{\text{cm}^2\,\text{s}} \qquad (141)$$

Eq. (141) gives the Incident Radiation sometimes also called spherical irradiance. Integration over the solid angle of irradiation eliminates the angular dependence of the transported radiation. For the one-dimensional - one directional model only integration on μ is required. The time dependence on G is not considered under the assumption that the optical properties of the catalyst remain constant. The LVRPA or the photon absorption rate as a function of position, results:

$$e_\lambda^a(x) = \kappa_\lambda\, G_\lambda(x) \quad [=] \quad \frac{\text{einstein}}{\text{cm}^3\,\text{s}} \qquad (142)$$

The absorption coefficient has been assumed independent of position (uniform catalyst concentration) and time (stable catalyst). The reactor volume average of the LVRPA for the one-dimensional model in the Cartesian coordinate x is:

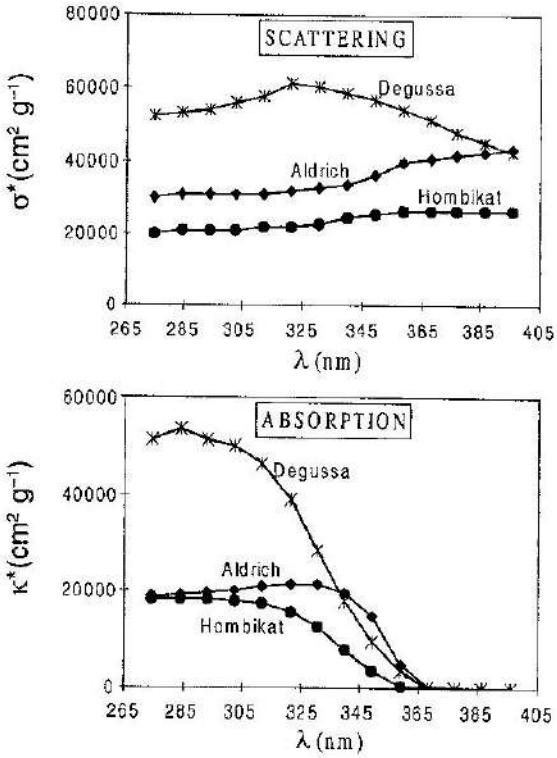

Fig. 15. Specific scattering and absorption coefficients of different brands of TiO_2. Adapted from [Cabrera et al., 1996; Cassano and Alfano, 2000].

Table N° 2

Variable	Value	Units
Wavelength	313 and 365	nm
Radiation intensity for 313 nm (at clean reactor window)	2.187×10^{-10}	einstein /cm^2 s sr
Radiation intensity for 365 nm (at clean reactor window)	4.997×10^{-10}	einstein /cm^2 s sr
Temperature	298	K
Initial pH	3.0	———
Initial substrate concentration	20	p.p.m.
Catalyst	Degussa P 25	
Catalyst concentration	2.0	g / L
Use pure substrates and pure water		
Work under zero order reaction rate regimes with respect to substrate and catalyst concentrations		

Table N° 3: Results

Compound	Quantum Yield (%) mol einstein^{-1}	
	λ = 313 nm	λ = 365 nm
Phenol	9.5	8.5
1,4-Dioxane	5.3	4.0

$$\left\langle e_\lambda^a \right\rangle_{V_R} = \frac{1}{L_R} \int_0^{L_R} e_\lambda^a(x)\, dx \qquad (143)$$

Equations (141) to (143) provides the denominator of Eq. (100).

VII.7. Results

Absolute values of the true monochromatic quantum yields have been recently measured for 1,4-dioxane and phenol [Cassano *et al.*, 2002]. The adopted standard conditions are described in Table N° 2.

Employing the method described in previous sections, the reported values are presented in Table N° 3.

It must be stressed that the approach shown here for calculating quantum yields is almost the same that must be used to design any slurry photocatalytic reactor. Moreover, these concepts can also be adapted and/or extended to design other photocatalytic reactor configurations (for example, fixed or fluidized bed operations).

Acknowledgments

The authors are grateful to Universidad Nacional del Litoral, Consejo Nacional de Investigaciones Científicas y Técnicas, Agencia Nacional de Promoción Científica y Tecnológica and the CYTED program for their support to produce this work. Thanks are also given to Eng. Claudia M. Romani for technical assistance.

References

Alfano, O. M., Romero, R. L. and Cassano A. E. A Cylindrical Photoreactor Irradiated From the Bottom. I. Radiation Flux Density Generated by a Tubular Source and a Parabolic Reflector, *Chem. Eng. Sci.*, 40, 2119-2127 (1985).

Alfano, O. M., Romero, R. L. and Cassano A. E. A Cylindrical Photoreactor Irradiated from the Bottom. II. Models for the Local Volumetric Rate of Energy Absorption with Polychromatic Radiation and their Evaluation, *Chem. Eng. Sci.*, 41, 1155-1161 (1986) (a).

Alfano, O. M., Romero, R. L., Negro C. A. and Cassano A. E. A Cylindrical Photoreactor Irradiated from the Bottom. III. Measurement of Absolute Values of the Local Volumetric Rate of Energy Absorption. Experiments with Polychromatic Radiation, *Chem. Eng. Sci.*, 41, 1163-1169 (1986) (b).

Alfano, O. M., Negro, A. C., Cabrera, M. I. and Cassano, A. E. Scattering Effects Produced by Inert Particles in Photochemical Reactors. 1. Model and Experimental Verifica-

tion, *Ind. Eng. Chem. Res.*, 34 (2), 488-499 (1995).

Alfano, O. M., Cabrera, M. I., and Cassano, A. E. Photocatalytic Reactions Involving Hydroxyl Radical Attack I: Reaction Kinetics Formulation with Explicit Photon Absorption Effects, *J. Catal.*, 172 (2), 370-379 (1997).

Bird, R. B., Stewart, W. E. and Lightfoot, E. N., *Transport Phenomena*, 2nd Edit., J. Wiley & Sons, New York, 2002.

Brandi, R. J., Alfano, O. M., and Cassano, A. E. Rigorous Model and Experimental Verification of the Radiation Field in a Flat Plate Solar Collector Simulator Employed for Photocatalytic Reactions, *Chem. Eng. Science*, 54 (13-14), 2817-2827 (1999).

Brandi, R. J., Alfano, O. M. and Cassano, A. E. Evaluation of Radiation Absorption in Slurry Photocatalytic Reactors. 1. Assessment of Methods in Use and New Proposal, *Environ. Sci. Technol.*, 34 (12), 2623-2630 (2000) (a).

Brandi, R. J., Alfano, O. M. and Cassano, A. E. Evaluation of Radiation Absorption in Slurry Photocatalytic Reactors. 2. Experimental Verification of the Proposed Method, *Environ. Sci. Technol.*, 34 (12), 2631-2639 (2000) (b).

Braun, A. M., Jakob, L., Oliveros, E. and Oller do Nascimento, C. A. Up-Scaling Photochemical Reactions, *Advances in Photochemistry*, 18, 235-313 (1993).

Cabrera, M. I., Alfano, O. M., and Cassano, A. E. Novel Reactor for Photocatalytic Kinetic Studies, *Ind. Eng. Chem. Res.*, 33 (12), 3031-3042 (1994).

Cabrera, M. I., Alfano, O. M., and Cassano, A. E. Absorption and Scattering Coefficients of Titanium Dioxide Particulate Suspensions in Water, *J. Phys. Chem.*, 100 (51), 20043-20050 (1996).

Cabrera, M. I., Martín, C. A., Alfano, O. M. and Cassano, A. E. Photochemical Decomposition of 2,4-Dichlorophenoxyacetic Acid (2,4-D) in Aqueous Solution. I. Kinetic Study, *Wat. Sci. Tech.*, 35 (4), 31-39 (1997) (a).

Cabrera, M. I., Negro, A. C., Alfano, O. M. and Cassano, A. E. Photocatalytic Reactions Involving Hydroxyl Radical Attack II: Kinetics of the Decomposition of Trichloroethylene using Titanium Dioxide, *J. Catal.*, 172 (2), 380-390 (1997) (b).

Cassano, A. E., Alfano, O. M. and Romero, R. L. Photoreactor Engineering: Analysis and Design, in *Concepts and Design of Chemical Reactors*; Whitaker, S., Cassano A. E., Gordon and Breach (Editor), New York, 339-512, 1986.

Cassano, A. E. and Alfano, O. M. Reaction Engineering of Suspended Solid Heterogeneous Photocatalytic Reactors, *Catal. Today*, 58 (2-3), 167-197 (2000).

Cassano, A. E., Brandi, R. J., Citroni, M. A. and Alfano, O. M. Photocatalysis in Slurry Reactors. A Proposal for Standard Values of True Quantum Yields, *ISCRE XVII*, Hon Kong (2002), submitted.

Cassano, A. E., Martín, C. A., Brandi, R. J., and Alfano, O. M. Photoreactor Analysis and Design: Fundamentals and Applications, *Ind. Eng. Chem. Res.*, 34 (7), 2155-2201 (1995).

Chiovetta, M. G., Romero R. L. and Cassano, A. E. Modeling of a Fluidized-Bed Photocatalytic Reactor for Water Pollution Abatement, *Chem. Eng. Science*, 56, 1631-1638 (2001).

Duderstadt, J. J., Martin, W. R. *Transport Theory*, J. Wiley (Editor), New York, 1979.

Froment, G. F. and Bischoff, K. B., *Chemical Reactor Analysis and Design*, 2nd Edit., J. Wiley & Sons (Edit.), New York, 1990.

Irazoqui, H. A., Cerdá, J., Cassano, A. E., Radiation Profiles in an Empty Annular Photoreactor with a Source of Finite Spatial Dimensions, *AIChE J.*, 19, 460-467 (1973).

Jacob, S. M. and Dranoff, J. S., Radial Scale-Up of Perfectly Mixed Photochemical Reactors, *Chem. Eng. Prog. Symposium Ser.*, 62 (68), 47-55 (1966).

Marquardt, D. W., *J. Soc. Indust. Appl. Math.* 11, 431-441 (1963).

Martín, C. A., Baltanás, M. A. and Cassano, A. E., Photocatalytic Reactors II. Quantum Efficiencies Allowing for Scattering Effects. An Experimental Approximation. *J. Photochem. Photobiol. A: Chem.*, 94, 173-189 (1996).

Martín, C. A., Cabrera, M. I., Alfano, O. M. and Cassano, A. E., Photochemical Decomposition of 2,4-Dichlorophenoxyacetic Acid (2,4-D) in Aqueous Solution. II. Reactor Modeling and Verification, *Wat. Sci. Tech.*, 35 (4), 197-205 (1997).

Murov, S. L., Carmichael, I., Hug, G. L., *Handbook of Photochemistry*, 2nd Edit., Marcel Dekker (Edit.), New York, 1993.

Ozisik, M. N., *Radiative Transfer and Interactions with Conduction and Convection*, Wiley (Edit), New York, 1973.

Puma, G. L. and Yue, P. L., A Laminar Falling Film Slurry Photocatalytic Reactor. Part I-Model Development, *Chem. Eng. Sci.*, 53, 2993-3006 (1998).

Ray, A. K., A New Photocatalytic Reactor for Destruction of Toxic Water Pollutants by Advanced Oxidation Process, *Catal. Today*, 44, 357-368 (1998).

Romero, R. L., Alfano, O. M. and Cassano, A. E., Cylindrical Photocatalytic Reactors. Radiation Absorption and Scattering Effects Produced by Suspended Fine Particles in an Annular Space, *Ind. Eng. Chem. Res.*, 36 (8), 3094-3109 (1997).

Romero, R. L., Alfano, O. M., Marchetti, J. L., Cassano, A. E., Modelling and Parametric Sensitivity of an Annular Photoreactor with Complex Kinetics, *Chem. Eng. Sci.*, 38, 1593-1605 (1983).

Siegel, R.; Howell, J. R. *Thermal Radiation Heat Transfer*, 3rd Edit., Hemisphere (Edit.), Washington, 1992.

van de Hulst, H. C., *Light Scattering by Small Particles*, Wiley (Edit.), New York, 1957.

Manuscrito recibido y aceptado en julio de 2002